Distribution and degradation trend of micropollutants in a surface flow treatment wetland revealed by 3D numerical modelling combined with LC-MS/MS

Loïc Maurer[a,b], Claire Villette[a], Nicolas Reiminger[b] , Xavier Jurado[b], Julien Laurent[b] , Maximilien Nuel, Robert Mosé[b], Adrien Wanko[b], Dimitri Heintz[a]

[a]Plant Imaging and Mass Spectrometry (PIMS), Institut de biologie moléculaire des plantes, CNRS, Université de Strasbourg, 12 rue du Général Zimmer, 67084 Strasbourg, France.

[b]Département mécanique, ICube Laboratoire des sciences de l'ingénieur, de l'informatique et de l'imagerie, UNISTRA/CNRS/ENGEES/INSA, 2 rue Boussingault, 67000 Strasbourg, France.

Corresponding author : Dimitri Heintz, dimitri.heintz@ibmp-cnrs.unistra.fr

---

Citation : Maurer, L., Villette, C., Reiminger, N., Jurado, X., Laurent, J., Nuel, M., Mosé, R., Wanko, A., & Heintz, D. (2021). Distribution and degradation trend of micropollutants in a surface flow treatment wetland revealed by 3D numerical modelling combined with LC-MS/MS. Water Research, 190, 116672. https://doi.org/10.1016/j.watres.2020.116672

Abstract: Conventional waste water treatment plants were not designed to treat micropollutants. For 20 years, these issues have led to several complementary treatment systems to deal with them, such as surface flow wetland. Previous studies have demonstrated that a higher residence time and global low velocities promote nutrient removal rates or micropollutants photodegradation. Nevertheless, these studies were restricted to the systems limits (inlet/outlet). Therefore, a detailed knowledge of water flow is crucial to identify areas promoting this degradation and to optimize these surface flow wetlands. The present study combines 3D water flow numerical modelling and liquid chromatography coupled to high resolution mass spectrometry (LC-HRMS/MS). Using this numerical model, validated by tracer experimental data, several velocity areas have been distinguished in the wetland. Four areas have been selected to investigate the waterflow influence and lead to the following results. On the one hand, micropollutants number and concentration are independent of the waterflow. This result could be due to several assumptions, such as the chronic exposure associated with the low Renoylds number. On the other hand, the potential degradation products (metabolites) were also assessed in the sludge to investigate the micropollutant biodegradation processes occurring in the wetland. These micropollutants metabolites or degradation products were detected in higher proportions (both number and concentration) in lower flow rate areas. Besides, these results were also related to higher amount of plants and microorganisms' metabolites in these areas, suggesting a higher biological activity promoting this degradation.

Keywords: Micropollutants, LC-HRMS/MS, CFD, water flow modelling, sludge.

Highlights:

- Micropollutants distribution assessed using water flow modelling and mass spectrometry
- Micropollutants parent compounds distribution is independent of flow velocities
- Micropollutants degradation is promoted in low flow rate areas
- Higher biological activity is observed in low flow rate areas

Graphical abstract

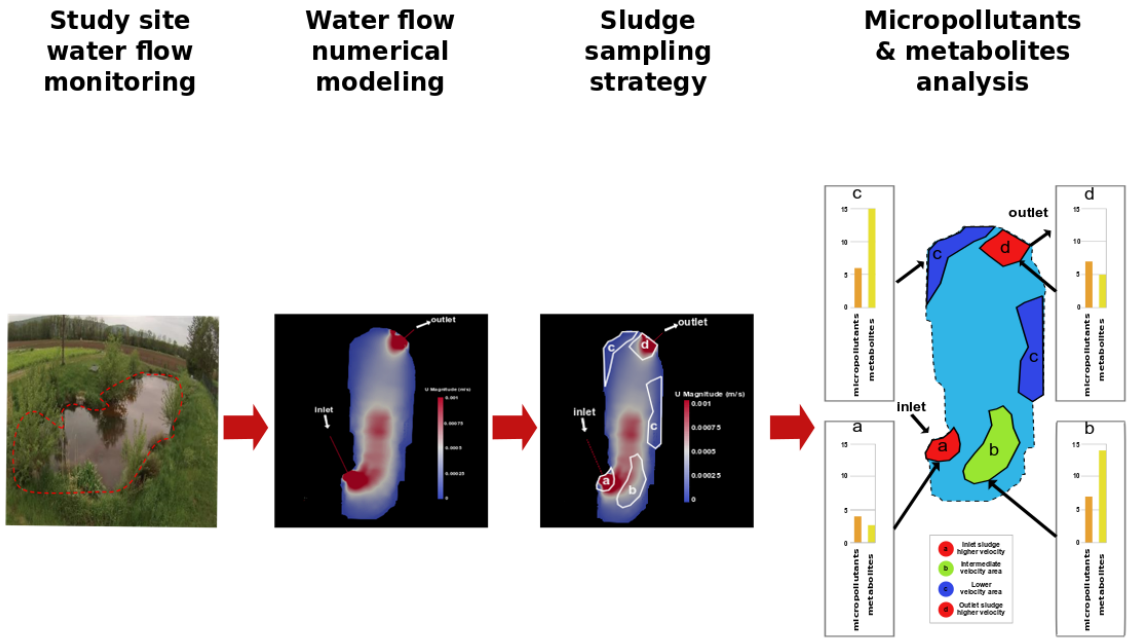

1. Introduction

In the past decades, water quality and micropollutants issues have become one of the major concerns in the water treatment field. Recent progress has confirmed this trend with the establishment of the Watch list in the European laws (Decision 2015/495/EU of 20 March 2015) (Barbosa et al., 2016; Mailler et al., 2017). Micropollutants found in the environment have several origins but urban wastewater is one of the most quoted (Kasprzyk-Hordern et al., 2009; Luo et al., 2014; Petrie et al., 2015; Phillips et al., 2012; Verlicchi et al., 2012). Indeed, a wide variety of our daily activities generate micropollutants, which end up in wastewater (washing, cooking, or drug consumption, etc.) and subsequently in wastewater treatment plants (WWTP). These wastewater treatment systems were not designed to treat micropollutants. Nevertheless, in the literature, waste water treatment systems and in particular constructed wetlands (CW) show their efficiency in the treatment of some micropollutants (Hijosa-Valsero et al., 2010; Matamoros and Bayona, 2006; Vymazal et al., 2017). In this way, part of the micropollutants can be caught by the different compartments of these systems whereas others are released into the environment. Besides, WWTPs are now also facing sustainability issues (reuse of water-derived resources and reduction of their environmental footprint) (Wang et al., 2015). Therefore, constructed wetlands and natural-based treatment systems seem to be well suited to these new challenges. In Europe these complementary treatment systems have been set up for 20 years and can improve micropollutant removal and reduce the impact of a direct release into the environment. Indeed, the WWTP set up could result in disturbing the environmental balance. For example, Tong et al., have mentioned the impact on nitrogen to phosphorus ratio in lakes found near the WWTP outlet (Tong et al., 2020). Surface flow treatment wetlands (SFTW) are particularly popular in rural communities (Mara et al., 1992). Indeed, they can offer several benefits such as complementary treatment for micropollutants, as it has been described in one of our previous studies (Nuel et al., 2018). Furthermore, the literature mentions hydraulics and specifically residence time as one of the major factors which could influence micropollutant removal (Boonnorat et al., 2016; Ejhed et al., 2018; Esperanza et al., 2007; Gros et al., 2010). The increase of residence time can promote different mechanisms useful in the management of micropollutants. For example, it is known that a longer residence time improves the biodegradation (Koch et al., 1999; Siegrist et al., 1995) of conventional pollutants such as nutrients. Concerning the micropollutants, photodegradation or sorption in sludge could be promoted by a higher residence time in this kind of system (Rühmland et al., 2015) and thus reduce their release into the environment. Nonetheless, most of the studies are focused on the system's boundary conditions (inlet/outlet) to characterize removal efficiency and compare global hydraulics parameters such as residence time distribution. But these global parameters could also hide the influence of specific areas inside water treatment systems. Therefore, a deep knowledge of hydraulics is crucial to understand the potential influence of water flow velocity on micropollutants distribution and degradation and would be useful to optimize the processes. Nonetheless, few studies have considered different regions inside a system to compare those which could influence the distribution or promote micropollutant removal (Gaullier et al., 2020). Among these studies, Mali et al., (2018) have used an 2D hydrodynamics model combined with passive scalar transport equation to determine metals distribution in a port. Their simulations show the influence of water flow velocity in this system. Another study conducted by Gaullier et al. (2020) has highlighted a heterogeneous distribution of pesticides in the constructed wetlands using tracer experiment in different water flow velocity areas. Nevertheless, this study did not consider the degradation process and therefore the fate of these pesticides was not fully investigated. As such, the aims of this study are to obtain a detailed knowledge of water flow velocities in a surface flow wetland and then to understand if these velocities could influence the micropollutants distribution and degradation. Therefore, we propose for the first time a 3D

surface wetland model based on a real study site geometry combined with a micropollutant large scale screening. This transient water flow model, validated by tracer experiment (comparison between experimental tracer experiment and simulation using passive scalar transport equation), was built to define the areas where sludge was collected. As sludge is a static compartment, micropollutants are sorbed according to their properties and to their affinity with solid; and can provide a general overview of the chronic micropollutant load. In this way, micropollutant analysis was linked to water flow process modelling to understand the potential influence of the water flow velocities field on micropollutant spatial distribution and degradation.

2. Materials and methods

2.1. Study site

The study site is a SFTW, located in Lutter (47°27'47.7"N 7°22'29.9"E; Grand Est, France) and implemented in 2009. The SFTW is a shallow-water pond with an impervious layer of clay in order to counter the high permeability of the natural soil. The SFTW has a surface of 750 m^2 with a maximal width of about 13 m, a maximal length of about 40 m, and having a heterogeneous depth. The SFTW has not yet been cleaned and mud has been accumulating since 2009. This SFTW was set up at the outlet of a two-stage vertical flow constructed wetland (VFCW) that collects wastewater (1000 people equivalent) before releasing it to SFTW and finally into the river. All the details concerning the SFTW could be found in Laurent et al., 2015.

2.2. Hydrodynamics numerical model

2.2.1. Water flow and passive scalar transport governing equations

CFD simulations were carried out on OpenFOAM 4.0, using the unsteady solver pimpleFoam. This solver was chosen for its ability to solve the Navier-Stokes equations in unsteady mode and considering incompressible and turbulent conditions for the flow resolution. Indeed, such turbulent conditions were observed in the SFTW inlet. The corresponding continuity [1] and momentum equations [2] are given below.

$$\nabla . u = 0 \quad [1]$$

$$\frac{\partial u}{\partial t} + u\,\nabla u = -\nabla p + \upsilon \Delta u \quad [2]$$

where u is the velocity, p the pressure, υ the kinematic viscosity and t the time. Due to calculation costs constraints, only water flow was considered in this study. On the other hand, a tracker simulation was performed to validate the model, considering the tracker as a passive scalar. The equation governing the passive scalar transport [3] is given below.

$$\frac{\partial C}{\partial t} + \nabla . (uC) - \nabla^2 (D_m C) = q_m \quad [3]$$

where C is the tracker concentration, u the velocity, t the time, D_m the tracker diffusion coefficient (sulforhodamine $D_m = 3.6\ 10^{-6}\ m^2/s$), and q_m the pollutant source term. To solve these equations a Reynolds-Averaged Navier-Stokes (RANS) method was used, with a turbulence closure scheme. The standard k-Ɛ model was selected for the turbulence as it is well adapted for large flow fields and it has been used in several cases of water flow simulations in ponds (Alvarado et al., 2013; Ouedraogo et al., 2016). The simulations were

performed using second order schemes. The results were extracted after convergence. All the simulation results were obtained with residuals lower than 10^{-7}.

2.2.2. Computational domains and boundary conditions

The CFD model geometry was built using data collected on the field. Indeed, all the surface points defining the limits of the computational domain were obtained using a GPS system. The domain was then split in 1-square-meter subdomains, and the depth was measured manually using a bathymetry approach. All these data were used to build a 3D geometry of the SFTW. An overview of the study site used for the 3D model can be found in Figure S1.
Regarding the boundary conditions, the following hypothesis was applied on the simulations. First, an inlet flow rate was defined for each simulation. The SFTW flow rate monitoring was performed using ultrasonic probes (IJINUS, MELLAC, France) and by built-in exponential section venturis (ISMA, Forbach, France) as described in Nuel et al. (Nuel et al., 2017). Then an average flow rate could be calculated and used for each simulation. This hypothesis can be applied as the difference between the maximum and minimum SFTW flow rate measurement was not significant according to the results obtained by Nuel et al. (Nuel et al., 2017). The outlet pressure was then considered at the outlet whereas no slip conditions were considered for the bank and the ground of the SFTW. Finally, symmetry conditions were used for the water surface. Considering the tracker experiment, an inlet mass flow rate was defined, with a mass flow rate of about 100 mg/s during the first 300 seconds of the simulation.
Subsequently the geometry was meshed. Mesh size was chosen in order to fulfill a Y^+ criterion between 30 and 300 (in accordance with criteria for the standard k-Ɛ model) according to the recommendations found in Versteeg et al. (Versteeg and Malalasekera, 2007). This Y^+ criterion was calculated following Equation [4]

$$\Delta s = \frac{\left(\frac{2}{0.026}\right)^{\frac{1}{2}} Y^+ \, \mu^{\frac{13}{14}}}{(\rho u)^{\frac{13}{14}} L^{-\frac{1}{14}}} \qquad [4]$$

where u is the averaged velocity m/s, ρ the water density ($kg.m^{-3}$), μ the dynamic viscosity ($kg.m^{-1}.s^{-1}$), L the average water depth (m) and Δs the mesh size in cm. Using this criteria, the recommended mesh size was between 1.1 and 11 cm. To reduce calculation cost, the mesh size selected was 10 cm.
This choice was checked during the model validation step. The model resulting from these choices has 1.5 million grid cells.

2.2.3. Model validation

The numerical model results were compared with the tracker experimental results obtained on the field to ensure both model and meshing validity. Indeed, tracer campaigns were performed with Sulforhodamine B (SRB, $C_{27}H_{29}N_2NaO_7S_2$) as a fluorescent dye, in order to estimate the SFTW residence time, as described in detail in Laurent et al. (Laurent et al., 2015). Briefly, an instantaneous pulse of tracer was injected at the inlet and the tracer concentrations were monitored by a fluorometer (GGUN-FL30, Albilia, Switzerland) connected to a peristaltic pump operating continuously at 1 $L.s^{-1}$. Fluorometer readings were calibrated on site by water samples collected at the same location and spiked with known tracer amounts.

Then these results were compared to numerical simulation using the passive scalar simulation described in Section 2.2.1. Alvarado et al. (Alvarado et al., 2013) and Coggins et al. (Coggins et al., 2017) have suggested the use of residence time to validate a SFTW water flow model. Figure S2 underlines the proper fit between the simulated and the experimental curves. In this way, the model can reproduce the outlet signal. According to the results, the model was validated for the rest of the study.

2.3. Chemicals

Acetic acid and formic acid were acquired from Sigma Aldrich (Missouri, USA). The extraction solvents (acetonitrile, methanol and isopropanol) were obtained from Fisher Chemicals (New Hampshire, USA). Ammonium formate was purchased from Fluka Analytical (Missouri, USA) and NaOH from Agilent Technologies (California, USA). Deionized water was obtained from a Direct-Q UV (Millipore) station. Finally, the internal standards used, namely bezafibrate–d4, diclofenac-d4, gemfibrozil-d6, N-desmethyl sildenafil-d8, sildenafil-d3, sulfamethoxazole-d4, were obtained from Toronto Research Chemical (Ontario, Canada) whereas the acetaminophen-d4 standard was purchased from Sigma Aldrich. These labelled internal standards were used to assess the repeatability of extraction process and to determine the limits of detection and quantification (Villette et al., 2019a). The commercial standards used for compounds quantification, namely irbesartan, oxadiazon, tramadol, etofenprox, celiprolol, desvenlafaxine, diflufenican, permethrin, propafenone, isoconazole, venlafaxine, fipronilulfone, acebutolol, amiodarone and climbazole, were purchased from Sigma Aldrich.

2.5. Micropollutants extraction

The micropollutants were analyzed in the sludge samples. Water flow modelling defines the sludge sampling strategy as described in Section 3. 1. In each area defined, a composite of surface sludge (the first ten cm) was collected (in each season), as this layer was directly in contact with the wastewater. The samples were stored at 4° C before the analysis. Then all the analyses were performed using 3 biological replicates. Micropollutants were extracted as described in Villette et al., 2019a. Briefly, 10 g of sludge were weighed, and a double extraction was carried out. The first overnight extraction was performed using 40 mL of acetonitrile:water (90:10) with 1% acetic acid at 4°C under shaking with a magnetic stirrer. The samples were centrifuged 15 min at 5500 rpm and the supernatant collected. Then a second extraction was carried out to the pellet using 20 mL of isopropanol:acetonitrile (90:10) during 15 min at 4°C under shaking. The samples were then centrifuged for 15 min at 5500 rpm, and the supernatant was recovered and freeze-dried. Finally, the samples were solubilized in 1 mL of acetonitrile:isopropanol:water (50:45:5). Parallel blank extraction was performed each season.

2.6. Micropollutants analysis

The samples were then analyzed in liquid chromatography (LC) coupled to high resolution mass spectrometry (HRMS), the method used being that mentioned in Villette et al., 2019a and Bergé et al., 2018, namely the TargetScreener method (Bruker). This method allows the targeted identification of drugs and pesticides but could also be investigated for non-targeted analysis. Briefly, a DioneX Utlimate 3000 (Thermo) coupled to a Q-TOF Impact II (Bruker) were used. The method operated with two solvents: solvent A: H2O:MeOH (90:10 v:v) with 0.01% formic acid and 314 mg.L-1 ammonium formate, and solvent B: MeOH with

0.01% formic acid and 314 mg.L-1 ammonium formate. The compounds were separated using a C18 column (Acclaim TM RSLC 120 C18, 2.2 µm 120A 2.1x100mm, Dionex bonded silica products) equipped with a C18 precolumn (Acquity UPLC ® C18, 1.7 µm, 2.1 × 5 mm). The compounds were analyzed using the spectrometer in positive ion mode with a spectra rate of 2 Hz, on a mass range from 30 to 1000 Da. Fragments were obtained using broad-band collision-induced dissociation (bbCID) with a MS/MS collision energy set at 30 eV. Analytical quality check was performed using a mix of pesticides to assess the retention time (refs 31972 and 31978 Restek). The detailed procedure and the operational parameters can be found in Villette et al. 2019a.

2.7. Data processing

The annotations for the LC-HRMS/MS data were performed using TASQ 1.4 (Bruker Daltonics). TASQ contains a database of 2204 drugs and pesticides injected, which has been used to annotate ions in targeted way based on the retention time, m/z value, the isotopic pattern of the parent ion (mSigma) and qualifier ions (daughter ion). . Using, this database, containing micropollutants commercial standards injected, all the identification could reach the level 1 from the Schymanski classification. The selection criteria were a signal-to-noise ratio higher than 3, a retention time variation lower than 0.3 min, an exact mass variation lower than 3 ppm and matching fragment ions when they were available. To obtain the most representative view of the contaminations, only micropollutants found in all seasons and in 3 biological replicates with commercial standards available were quantified. The mean concentration was determined using all the replicates and the standard deviation represent the variation found in the different seasons for each replicate. In addition, predicted catabolites and conjugates (metabolites) of these micropollutants were also annotated using in silico predictions performed in Metabolite Predict 2.0 (Bruker, Germany) (Pelander et al., 2009). This annotation process has already been described in Villette et al., 2019b. Briefly, 79 biotransformation rules were applied on the structure of the parent drugs to generate metabolites over two generations. The software then generated a list of raw formulae containing the potential metabolites but also retrieved the enzymes generating the metabolites. Finally, raw formulae lists were imported in Metaboscape 4.0. for annotation, in order to carry out suspect screening of these metabolites. The data are compared with, raw formulae generated using SmartFormula as mentioned in Villette et al., 2019b. The metabolites mentioned in this study were only those found in all season and in 3 biological replicates.

Finally, these data were also analyzed using a non-targeted way following the processing mentioned in Villette et al., 2019a. The annotations were carried out using a criterion of mass deviation lower than 3 ppm and mSigma value under 30 to assess the good fit of the isotope pattern. Then raw formula annotations were generated using C, H, N, O, P, S, Cl, I, Br and F elements. Then tentative identification (level 3 of the Schymanski classification (Schymanski et al., 2015) were obtained using analyte lists created from the toxic exposome database (http://www.t3db.ca/), FooDB (http://foodb.ca/), EU Reference Laboratories for Residues of Pesticides (http://www.eurl-pesticides.eu), Phenol Explorer (http://phenol-explorer.eu/), Scientific Working Group for the Analysis of Seized Drugs (http://www.swgdrug.org/), Norman Network (https://www.norman-network.net/), PlantCyc (https://www.plantcyc.org/), KNapSAcK (http://kanaya.naist.jp/KNApSAcK/) and SwissLipids (http://www.swisslipids.org/). In addition, these metabolites were analyzed using a statistical enrichment approach that is based on chemical similarity with the online ChemRICH tool (http://chemrich.fiehnlab.ucdavis.edu/) (Barupal and Fiehn, 2017). All the chemical identifiers (SMILES, PubChem ID and InChIKey) were manually collected using the PubChem Identifier Exchanger tool

(https://pubchem.ncbi.nlm.nih.gov/idexchange/idexchange.cgi). The identifiers have been used to evaluate the structural similarity between the compounds based on chemical ontologies.
Besides the compounds were also described using metabolic pathways. These metabolic networks were created using MetaMapp online tool (http://metamapp.fiehnlab.ucdavis.edu/ocpu/library/MetaMapp2020/www/) (Barupal et al., 2012). The chemical identifiers were kept from ChemRICH analysis and Kegg identifiers were manually searched in the Kegg database (https://www.genome.jp/kegg/), PubChem ID, SMILES and MetaMapp Then the software Cytoscape 3.8.0 was used to draw the different networks and biological pathways.

2.8. Statistical analysis

All the samples were replicated three times. In the non-target way, each area was analyzed separately, and the samples were clustered in Metaboscape 4.0 (Bruker Daltonics) according to the seasons and all the adducts form were grouped in a bucket. Briefly, using the value count of group attribute, only compounds found in 80% of group samples (water flow areas) were selected. The metabolic profile has therefore been investigated by comparing area by area based on a Wilcoxon rank sum test (non-parametric test). Results were considered significantly different using the fold change differences ≥ 2 or ≤ - 2 and the p-value <0.05. The fold change (associated to the different couples) and the associated p-value were recovered for use in ChemRICH. The whole dataset (statistically differential and non-differential values) was submitted to ChemRICH, with the fold change converted to average ratio. ChemRICH thresholds are p-value ≤ 0.05 and fold change ≥ 2 or ≤ -2 to consider that a compound is significantly up- or down-regulated in a specific condition (here, the pond) and to obtain the chemical enrichment analysis results.

3.Results

3.1. Water flow process modelling and areas selection

The SFTW was impacted by weather conditions; thus, different inlet flow rates were measured. The distribution of these inlet flow rates measured during 8 campaigns over 2 years is found in Figure S3. Among these flow rates, one inlet flow rate condition per season (Figure 1) was simulated to underline the water flow velocities field diversity that could be observed on the SFTW. The 3 slowest flow rates (winter with 7.2 m^3/h, summer with 5.1 m^3/h and autumn with 4.2 m^3/h) simulations induced a similar hydraulic behavior. Indeed, a preferential flow between the inlet and the outlet was noticed. The increase of the inlet flow rate can generate vortices (simulation A in Figure 1) and then the inlet-outlet link is no longer obvious. Nevertheless, Figure S3 highlights the extreme nature of this phenomenon. Therefore, the spring simulation (simulation A in Figure 1) in which vortices appear, was excluded for the rest of the study. The similar water flow behavior observed in the three other simulations provided a global overview of the SFTW hydraulics behavior. Even if a slow flow rate was set up at the SFTW inlet, some diversities could be observed. Indeed, the water flow velocities field seems to be particularly low near the banks in comparison to the other SFTW areas. On the other hand, a relatively higher water flow can be noticed near the inlet and outlet. While a low inlet flow rate is always detected in the SFTW, areas could be clustered as areas where water will perpetually flow (inlet, outlet and the preferential flow) and others where water will hardly ever flow (areas near the banks).

According to the three lowest flow rate simulations found in Figure 1, a sampling strategy was defined to collect sludge samples in the different flow rate areas. Four areas were selected, depicted in Figure 2. The main points of the water treatment system with relatively higher and perpetual flow was selected: the inlet (area a) and outlet (area d). In order to overcome these boundary conditions, two areas were chosen considering the water flows heterogeneity inside the SFTW. Therefore, sludge was collected in an area with an intermediate higher and perpetual flow rate, defined in Figure 2 as area b, and in areas near the banks with very low flow rate defined as area c. These areas were used for different seasonal sampling campaigns to analyze micropollutants and understand the influence of the flow rate on micropollutants presence in sludge.

3.2. Distribution of identified micropollutants according to the water flow areas.

The micropollutants analysis was performed for each season in the areas of interest for which the results are given in Figure S4 and Dataset 1. The micropollutants distribution fluctuates according to the season and does not seem to be related to the water flow. To overcome the seasonal effect and obtain a global overview, only the compounds found in all seasons were considered. The results are found in Figure 3. This general analysis indicates that the number of micropollutants found in the different sampling areas seems to be similar. Indeed 7 micropollutants were found in areas b and d, 6 in area c and 4 in area a. In addition, most of the compounds are found in at least 2 sampling areas, even if some micropollutants are only detected in a single area. Indeed, more than half of the micropollutants detected (100% in area a, 71% in area b and d, and 67% in area c) are found at least in two areas. Concerning their concentration, most of the micropollutants were found with concentrations between 40 and 400 µg/kg of sludge. Besides, little variations in concentrations can be noticed between the different areas where they were detected. For example, irbesartan was detected with concentrations between 76 and 125 µg/kg. Only celiprolol seems to be found in higher concentration in area c (491 µg/kg in area a and 1187 µg/kg in area c).

3.3. Distribution of micropollutants metabolites in the different water flow areas

Studies show that the analysis of parent compounds alone underestimates micropollutants amounts found in the environment. Indeed metabolites (potential conjugates or degradation products) could be found in higher quantities than parent compounds (Yin et al., 2017). Therefore, micropollutants metabolites (predicted derivatives) were also analyzed for each season in the areas of interest. The results are found in Figure S4 and Dataset 2. A similar trend can be found in the different seasons with a higher number of metabolites in relatively low water flow areas (b, c). This general trend is highlighted by the compounds found in all seasons in Figure 4. This global overview indicates that more compounds are identified in the lower flow rate areas (14 in area b and 15 in area c) than in the higher flow rate areas (4 in area a and 6 in area d). Besides, very few compounds are common to the different areas and a wide variety of metabolites intensities can be noticed. On the other hand, several drugs and their metabolites were studied, as shown in Figure 5. Indeed, tramadol and venlafaxine metabolites were found in higher amounts. A higher diversity in area c and irbesartan metabolites in area b, could be noticed suggesting that the lower flow rate influences the metabolization. However, the numbers of metabolites detected are not necessarily related to the amounts of the parent compounds. As a matter of fact, the numbers of metabolites are positively correlated for the tramadol (higher numbers of metabolites when the tramadol is not detected) whereas the opposite phenomenon was observed for the venlafaxine (higher numbers of metabolites when venlafaxine concentration is about 123 µg/kg sludge).

4.Discussion

4.1. Influence of boundary conditions

Figures 1 and 2 highlight the low velocity field in the SFTW. This low velocity field could be due to several phenomena, such as the low inlet flow rates compared to the pond sizes, the head losses resulting from the presence of vegetation, shallow depth and the rough sides. The influence of water depth has already been investigated by Coggins et al., with their study focused on the impact of sludge accumulation on the hydraulic performance (Coggins et al., 2017). Thus, it is not surprising that the areas of the SFTW that contain the most accumulated sludge and the areas near the banks are those with the lowest flow velocities field. These areas are characterized with a very high hydraulic residence time and consequently a low solid transport phenomenon. However, studies have shown that the water quality with higher nutrient removal (nitrogen and phosphorus) could be improved by increasing residence time (Akratos and Tsihrintzis, 2007; Huang, 2000). On the other hand, higher water flow velocity field can be noticed at the boundary points of the systems (inlet and outlet area) due to the boundary conditions (constrictions), hence leading to a high level of sludge renewable rate.

4.2. No correlation between parent compounds distribution and water flow velocities

The micropollutant analysis performed in the different areas does not highlight significant differences concerning their number and concentration, except for celiprolol. Indeed, almost the same number of micropollutants and similar concentration were found in the areas. However, according to the literature, sedimentation and sequestration of compounds in the solid phase should be promoted in lower water flow velocities field (Montiel-León et al., 2019). These comments are supported by studies that have investigated the influence of water flow velocities on contaminant concentrations and sequestration (Gaullier et al., 2020; Mali et al., 2018). Gaullier et al., (2020) suggested that the higher pesticides storage in the lower velocities areas is related to the transport types (convection is promoted in high velocity areas). On the other hand, Mali et al. underline a higher metal deposition in weaker flow in a port (Mali et al., 2018). Nevertheless, the higher velocities mentioned in their study will impact the flow patterns and could partly explained the differences.

Therefore, in our study, using the deep knowledge of water flow in treatment system, water flow velocities fields are not the key parameters governing the micropollutants distribution. The difference in water velocities is probably not significant to lead to a specific micropollutants distribution. Indeed, the Reynolds number found in the SFTW is low and the flow observed in the SFTW is generally laminar or low turbulent (except at the inlet and outlet) reducing the velocity difference in the areas. This trend is confirmed by the analysis of the areas of xenobiotics putatively identified in all the sampling areas found in Figure S6. This broader view highlights that most of the micropollutants are found in similar proportions in the different areas (fold change <2 (absolute value)). In addition, the study of physicochemical properties (log Kow, solubility, pka) as mentioned in Li et al., 2019 (Li et al., 2019), does not underline any correlation between micropollutants detection and these properties.

However, the impact of water flow velocity could probably be highlighted by other assumptions, such as solid transport or higher inlet flow rate. Indeed, a higher inlet flow rate would probably help to distinguish areas based on their micropollutants composition. If velocity differences between SFTW areas are increased, sequestration could be affected. However, all the results found for these micropollutants should be tempered with the

distribution of all the putative identifications coming from the non-targeted analysis, found in Figure S7. The general trend underlines that the low flow rate area (area c) seems to accumulate slightly more xenobiotics but also plant metabolites than other areas. These results seem to be more coherent with those found in the literature.

Another assumption which may explain this lack of differences (in concentration or area) could also be related to parent compounds degradation. Indeed, a higher sedimentation is probably occurring in the lower flow rate areas. But this sedimentation should be hidden by the degradation, which has also been enhanced in these areas.

4.3. *In situ* low water flow areas promote micropollutants degradation

A previous study has shown that parent compounds could be found in minor amounts compared to their metabolites (Yin et al., 2017). This degradation process could not be neglected in SFTW, as micropollutant biodegradation with conjugations and deconjugations has already been described in this kind of system (Tiwari et al., 2017). In our study, the distribution of micropollutants metabolites seems to be mainly influenced by the water flow. In fact, more biotransformation products are found in the areas where water hardly flows (14 in area b and 15 in area c versus 4 and 6 in areas a and d respectively). However, these areas, where water hardly flows are not located in the main water flow channel and could be subject to intermittent flow. Rožman et al. underline that a system with intermittent water flow provides a higher biodegradation capacity than permanent water flow, due to the biofilm development (Rožman et al., 2018). These conclusions support our observations. Besides, the areas with higher residence time can provide conditions stimulating degradation, such as an increase of the potential contact time with microorganisms. And the influence of a prolonged contact time in a bioreactor to improve micropollutants transformation has already been demonstrated (Asif et al., 2018; Boonnorat et al., 2016).

Similarly, the results found in Figure 5 suggest that the higher numbers of micropollutants metabolites in the lower flow rate areas (b and c), is not necessarily related to the numbers of parent compounds. Other phenomena such as metabolites transport could also occur. By analyzing the data using a broader view, the metabolites distribution still seems to follow a general trend. Indeed, with a closer look at their elemental composition, compounds with less than 15 or 10 carbons show the same distribution as the one described for micropollutants metabolites (Figure S8). The lower flow rate areas (b or c) seem to stimulate compound deposition and transformation. Besides, these conditions promoting biodegradation could also be pointed out with the non-target analysis and the chemical classes investigation using ChemRICH (Barupal and Fiehn, 2017) as shown in Figure S9. The results underline a specific detection of alkaloids and monoterpenes in the lower velocities areas. These observations are not surprising as plants grow near the wetland banks. In addition, phosphatidylethanolamines, main component of the bacterial membrane, have also been detected. Therefore, the compound annotations seem to indicate higher biological activities combining plants and microorganisms in these areas. Furthermore, the investigation of the networks and the biological pathways detected in the different areas, as described in Figure S10, could also suggest a higher biological activity in lower velocities areas. By comparing, the networks found in the lower water flow area (c) to higher water flow area (a or d), complex relationships are mainly observed in the lower velocities area. The network data also show that succinate is mainly found in the low flow rate area. Nguyen et al. have demonstrated that the bacteria feeding by this succinate could improve the energetic efficiency and lead to a higher drug (sulfomethoxazole) removal rate (Nguyen et al., 2017). On the other hand, this activity could also be pointed out with the p-cymene

detection. Indeed, this compound could be considered as a biogas marker but also as a part of an anaerobic digestion. (Moreno et al., 2014)

Finally, a general biodegradation process seems to occur in the SFTW. Indeed, most of the metabolites found (59%) seem to be generated according to a biodegradation process using cytochrome P450 hydroxylation or epoxidation followed by different transferase, dehydrogenase, hydrolase, esterase activities, as shown in Figure S11. It is well documented that cytochromes P450 have a key role in the Phase I metabolism for several herbicides (Cañameras et al., 2015). Also, cytochrome P450, found in several organisms, can degrade a wide variety of micropollutants due to their low specificity (Cañameras et al., 2015), and could explained this general process. This study was restricted to the biodegradation, but other abiotic processes could also be considered to understand the fate of micropollutants in the SFTW, such as such as photodegradation, or environmental conditions, (pH, redox), (De Laurentiis et al., 2012; Ávila et al., 2013; Lee et al., 2014; Rühmland et al., 2015).

5.Conclusion

The results found in this manuscript underline that the locally lower water flow velocities areas seem to influence the micropollutants degradation in SFTW wetland. A deep knowledge of the hydraulic behavior in the SFTW has been obtained through a 3D model based on the real study site geometry. Nonetheless, the micropollutant (parent compounds) distribution was independent from the locally heterogeneous water flow velocities. This independence could be partly explained by the model assumptions (transport solid or abiotic transformation were not evaluated in this study). Nevertheless, these hypotheses should be balanced with the results of micropollutant metabolites. As a matter of fact, metabolites can be found in higher amounts and are more representative of this pollution distribution. Indeed, these metabolites are found in higher proportion in lower flow rate areas than in faster flow rate areas. Therefore, low flow rate conditions seem to promote degradation; as such, the velocity differences have an impact on metabolites distribution. Unlike parent compounds, it seems that metabolites are mainly found in specific areas where environmental conditions generate micropollutant degradation. Indeed, these areas also accumulated a higher number of microorganisms or plants metabolites, indicating a higher biological activity. The analysis of small molecules (molecular formula comprising less than 15 or 10 carbons) distribution in the SFTW could also supported this observation. Consequently, a comparison with different systems operating in different geographical areas and with different flow rates and the investigation of non-biotic processes should be performed to strengthen these results.

Acknowledgments

We acknowledge the Agence de l'Eau Rhin Meuse (AERM) and the village of Lutter for the access to the SFTW.

Author Contributions

Loïc Maurer performed the CFD modelling, sample preparation, data analysis, prepared the figure, designed the research and wrote the manuscript. Claire Villette performed the LC-Q-TOF-HRMS/MS data acquisition and discussed the manuscript. Nicolas Reiminger, Xavier Jurado and Julien Laurent participated in CFD modelling and discussed the manuscript. Adrien Wanko discussed the manuscript. Maximilien Nuel performed the water flow monitoring on the study site. Robert Mosé discussed the manuscript. Dimitri Heintz discussed the manuscript and designed the research.

References

Akratos, C.S., Tsihrintzis, V.A., 2007. Effect of temperature, HRT, vegetation and porous media on removal efficiency of pilot-scale horizontal subsurface flow constructed wetlands. Ecological Engineering 29, 173–191. https://doi.org/10.1016/j.ecoleng.2006.06.013

Alvarado, A., Vesvikar, M., Cisneros, J.F., Maere, T., Goethals, P., Nopens, I., 2013. CFD study to determine the optimal configuration of aerators in a full-scale waste stabilization pond. Water Research 47, 4528–4537. https://doi.org/10.1016/j.watres.2013.05.016

Asif, M.B., Hai, F.I., Dhar, B.R., Ngo, H.H., Guo, W., Jegatheesan, V., Price, W.E., Nghiem, L.D., Yamamoto, K., 2018. Impact of simultaneous retention of micropollutants and laccase on micropollutant degradation in enzymatic membrane bioreactor. Bioresource Technology 267, 473–480. https://doi.org/10.1016/j.biortech.2018.07.066

Ávila, C., Reyes, C., Bayona, J.M., García, J., 2013. Emerging organic contaminant removal depending on primary treatment and operational strategy in horizontal subsurface flow constructed wetlands: Influence of redox. Water Research 47, 315–325. https://doi.org/10.1016/j.watres.2012.10.005

Barbosa, M.O., Moreira, N.F.F., Ribeiro, A.R., Pereira, M.F.R., Silva, A.M.T., 2016. Occurrence and removal of organic micropollutants: An overview of the watch list of EU Decision 2015/495. Water Research 94, 257–279. https://doi.org/10.1016/j.watres.2016.02.047

Barupal, D.K., Fiehn, O., 2017. Chemical Similarity Enrichment Analysis (ChemRICH) as alternative to biochemical pathway mapping for metabolomic datasets. Scientific Reports 7, 14567. https://doi.org/10.1038/s41598-017-15231-w

Barupal, D.K., Haldiya, P.K., Wohlgemuth, G., Kind, T., Kothari, S.L., Pinkerton, K.E., Fiehn, O., 2012. MetaMapp: mapping and visualizing metabolomic data by integrating information from biochemical pathways and chemical and mass spectral similarity. BMC Bioinformatics 13, 99. https://doi.org/10.1186/1471-2105-13-99

Bergé, A., Buleté, A., Fildier, A., Mailler, R., Gasperi, J., Coquet, Y., Nauleau, F., Rocher, V., Vulliet, E., 2018. Non-target strategies by HRMS to evaluate fluidized micro-grain activated carbon as a tertiary treatment of wastewater. Chemosphere 213, 587–595. https://doi.org/10.1016/j.chemosphere.2018.09.101

Boonnorat, J., Techkarnjanaruk, S., Honda, R., Prachanurak, P., 2016. Effects of hydraulic retention time and carbon to nitrogen ratio on micro-pollutant biodegradation in membrane bioreactor for leachate treatment. Bioresource Technology 219, 53–63. https://doi.org/10.1016/j.biortech.2016.07.094

Cañameras, N., Comas, J., Bayona, J.M., 2015. Bioavailability and Uptake of Organic Micropollutants During Crop Irrigation with Reclaimed Wastewater: Introduction to Current Issues and Research Needs, in: Fatta-Kassinos, D., Dionysiou, D.D., Kümmerer, K. (Eds.), Wastewater Reuse and Current Challenges, The Handbook of Environmental Chemistry. Springer International Publishing, Cham, pp. 81–104. https://doi.org/10.1007/698_2015_412

Coggins, L.X., Ghisalberti, M., Ghadouani, A., 2017. Sludge accumulation and distribution impact the hydraulic performance in waste stabilisation ponds. Water Research 110, 354–365. https://doi.org/10.1016/j.watres.2016.11.031

De Laurentiis, E., Chiron, S., Kouras-Hadef, S., Richard, C., Minella, M., Maurino, V., Minero, C., Vione, D., 2012. Photochemical Fate of Carbamazepine in Surface Freshwaters: Laboratory Measures and Modeling. Environ. Sci. Technol. 46, 8164–8173. https://doi.org/10.1021/es3015887

Ejhed, H., Fång, J., Hansen, K., Graae, L., Rahmberg, M., Magnér, J., Dorgeloh, E., Plaza, G., 2018. The effect of hydraulic retention time in onsite wastewater treatment and removal of pharmaceuticals, hormones and phenolic utility substances. Science of The Total Environment 618, 250–261. https://doi.org/10.1016/j.scitotenv.2017.11.011

Esperanza, M., Suidan, M.T., Marfil-Vega, R., Gonzalez, C., Sorial, G.A., McCauley, P., Brenner, R., 2007. Fate of sex hormones in two pilot-scale municipal wastewater treatment plants: Conventional treatment. Chemosphere 66, 1535–1544. https://doi.org/10.1016/j.chemosphere.2006.08.020

Gaullier, C., Dousset, S., Baran, N., Kitzinger, G., Coureau, C., 2020. Influence of hydrodynamics on the water pathway and spatial distribution of pesticide and metabolite concentrations in constructed wetlands. Journal of Environmental Management 270, 110690. https://doi.org/10.1016/j.jenvman.2020.110690

Gros, M., Petrović, M., Ginebreda, A., Barceló, D., 2010. Removal of pharmaceuticals during wastewater treatment and environmental risk assessment using hazard indexes. Environment International 36, 15–26. https://doi.org/10.1016/j.envint.2009.09.002

Hijosa-Valsero, M., Matamoros, V., Martín-Villacorta, J., Bécares, E., Bayona, J.M., 2010. Assessment of full-scale natural systems for the removal of PPCPs from wastewater in small communities. Water Research 44, 1429–1439. https://doi.org/10.1016/j.watres.2009.10.032

Huang, J., 2000. Nitrogen removal in constructed wetlands employed to treat domestic wastewater. Water Research 34, 2582–2588. https://doi.org/10.1016/S0043-1354(00)00018-X

Kasprzyk-Hordern, B., Dinsdale, R.M., Guwy, A.J., 2009. The removal of pharmaceuticals, personal care products, endocrine disruptors and illicit drugs during wastewater treatment and its impact on the quality of receiving waters. Water Research 43, 363–380. https://doi.org/10.1016/j.watres.2008.10.047

Koch, G., Pianta, R., Krebs, P., Siegrist, H., 1999. Potential of denitrification and solids removal in the rectangular clarifier. Water Research 33, 309–318. https://doi.org/10.1016/S0043-1354(98)00220-6

Laurent, J., Bois, P., Nuel, M., Wanko, A., 2015. Systemic models of full-scale Surface Flow Treatment Wetlands: Determination by application of fluorescent tracers. Chemical Engineering Journal 264, 389–398. https://doi.org/10.1016/j.cej.2014.11.073

Lee, E., Shon, H.K., Cho, J., 2014. Role of wetland organic matters as photosensitizer for degradation of micropollutants and metabolites. Journal of Hazardous Materials 276, 1–9. https://doi.org/10.1016/j.jhazmat.2014.05.001

Li, Y., Sallach, J.B., Zhang, W., Boyd, S.A., Li, H., 2019. Insight into the distribution of pharmaceuticals in soil-water-plant systems. Water Research 152, 38–46. https://doi.org/10.1016/j.watres.2018.12.039

Luo, Y., Guo, W., Ngo, H.H., Nghiem, L.D., Hai, F.I., Zhang, J., Liang, S., Wang, X.C., 2014. A review on the occurrence of micropollutants in the aquatic environment and their fate and removal during wastewater treatment. Science of The Total Environment 473–474, 619–641. https://doi.org/10.1016/j.scitotenv.2013.12.065

Mailler, R., Gasperi, J., Patureau, D., Vulliet, E., Delgenes, N., Danel, A., Deshayes, S., Eudes, V., Guerin, S., Moilleron, R., Chebbo, G., Rocher, V., 2017. Fate of emerging and priority micropollutants during the sewage sludge treatment: Case study of Paris conurbation. Part 1: Contamination of the different types of sewage sludge. Waste Management 59, 379–393. https://doi.org/10.1016/j.wasman.2016.11.010

Mali, M., Malcangio, D., Dell' Anna, M.M., Damiani, L., Mastrorilli, P., 2018. Influence of hydrodynamic features in the transport and fate of hazard contaminants within touristic ports. Case study: Torre a Mare (Italy). Heliyon 4, e00494. https://doi.org/10.1016/j.heliyon.2017.e00494

Mara, D.D., Mills, S.W., Pearson, H.W., Alabaster, G.P., 1992. Waste Stabilization Ponds: A Viable Alternative for Small Community Treatment Systems. Water and Environment Journal 6, 72–78. https://doi.org/10.1111/j.1747-6593.1992.tb00740.x

Matamoros, V., Bayona, J.M., 2006. Elimination of Pharmaceuticals and Personal Care Products in Subsurface Flow Constructed Wetlands. Environmental Science & Technology 40, 5811–5816. https://doi.org/10.1021/es0607741

Montiel-León, J.M., Munoz, G., Vo Duy, S., Do, D.T., Vaudreuil, M.-A., Goeury, K., Guillemette, F., Amyot, M., Sauvé, S., 2019. Widespread occurrence and spatial distribution of glyphosate, atrazine, and neonicotinoids pesticides in the St. Lawrence and tributary rivers. Environmental Pollution 250, 29–39. https://doi.org/10.1016/j.envpol.2019.03.125

Moreno, A.I., Arnáiz, N., Font, R., Carratalá, A., 2014. Chemical characterization of emissions from a municipal solid waste treatment plant. Waste Management 34, 2393–2399. https://doi.org/10.1016/j.wasman.2014.07.008

Nguyen, P.Y., Carvalho, G., Reis, A.C., Nunes, O.C., Reis, M.A.M., Oehmen, A., 2017. Impact of biogenic substrates on sulfamethoxazole biodegradation kinetics by Achromobacter denitrificans strain PR1. Biodegradation 28, 205–217. https://doi.org/10.1007/s10532-017-9789-6

Nuel, M., Laurent, J., Bois, P., Heintz, D., Mosé, R., Wanko, A., 2017. Seasonal and ageing effects on SFTW hydrodynamics study by full-scale tracer experiments and dynamic time warping algorithms. Chemical Engineering Journal 321, 86–96. https://doi.org/10.1016/j.cej.2017.03.013

Nuel, M., Laurent, J., Bois, P., Heintz, D., Wanko, A., 2018. Seasonal and ageing effect on the behaviour of 86 drugs in a full-scale surface treatment wetland: Removal efficiencies and distribution in plants and sediments. Science of The Total Environment 615, 1099–1109. https://doi.org/10.1016/j.scitotenv.2017.10.061

Ouedraogo, F.R., Zhang, J., Cornejo, P.K., Zhang, Q., Mihelcic, J.R., Tejada-Martinez, A.E., 2016. Impact of sludge layer geometry on the hydraulic performance of a waste stabilization pond. Water Research 99, 253–262. https://doi.org/10.1016/j.watres.2016.05.011

Pelander, A., Tyrkkö, E., Ojanperä, I., 2009. *In silico* methods for predicting metabolism and mass fragmentation applied to quetiapine in liquid chromatography/time-of-flight mass spectrometry urine drug screening. Rapid Commun. Mass Spectrom. 23, 506–514. https://doi.org/10.1002/rcm.3901

Petrie, B., Barden, R., Kasprzyk-Hordern, B., 2015. A review on emerging contaminants in wastewaters and the environment: Current knowledge, understudied areas and recommendations for future monitoring. Water Research 72, 3–27. https://doi.org/10.1016/j.watres.2014.08.053

Phillips, P.J., Chalmers, A.T., Gray, J.L., Kolpin, D.W., Foreman, W.T., Wall, G.R., 2012. Combined Sewer Overflows: An Environmental Source of Hormones and Wastewater Micropollutants. Environmental Science & Technology 46, 5336–5343. https://doi.org/10.1021/es3001294

Rožman, M., Acuña, V., Petrović, M., 2018. Effects of chronic pollution and water flow intermittency on stream biofilms biodegradation capacity. Environmental Pollution 233, 1131–1137. https://doi.org/10.1016/j.envpol.2017.10.019

Rühmland, S., Wick, A., Ternes, T.A., Barjenbruch, M., 2015. Fate of pharmaceuticals in a subsurface flow constructed wetland and two ponds. Ecological Engineering 80, 125–139. https://doi.org/10.1016/j.ecoleng.2015.01.036

Schymanski, E.L., Singer, H.P., Slobodnik, J., Ipolyi, I.M., Oswald, P., Krauss, M., Schulze, T., Haglund, P., Letzel, T., Grosse, S., 2015. Non-target screening with high-resolution mass spectrometry: critical review using a collaborative trial on water analysis. Analytical and bioanalytical chemistry 407, 6237–6255.

Siegrist, H., Krebs, P., Bühler, R., Purtschert, I., Rock, C., Rufer, R., 1995. Denitrification in secondary clarifiers. Water Science and Technology, Modelling and Control of Activated Sludge Processes 31, 205–214. https://doi.org/10.1016/0273-1223(95)00193-Q

Tiwari, B., Sellamuthu, B., Ouarda, Y., Drogui, P., Tyagi, R.D., Buelna, G., 2017. Review on fate and mechanism of removal of pharmaceutical pollutants from wastewater using biological approach. Bioresource Technology 224, 1–12. https://doi.org/10.1016/j.biortech.2016.11.042

Tong, Y., Wang, M., Peñuelas, J., Liu, X., Paerl, H.W., Elser, J.J., Sardans, J., Couture, R.-M., Larssen, T., Hu, H., Dong, X., He, W., Zhang, W., Wang, X., Zhang, Y., Liu, Y., Zeng, S., Kong, X., Janssen, A.B.G., Lin, Y., 2020. Improvement in municipal wastewater treatment alters lake nitrogen to phosphorus ratios in populated regions. Proc Natl Acad Sci USA 117, 11566–11572. https://doi.org/10.1073/pnas.1920759117

Verlicchi, P., Al Aukidy, M., Zambello, E., 2012. Occurrence of pharmaceutical compounds in urban wastewater: Removal, mass load and environmental risk after a secondary treatment—A review. Science of The Total Environment 429, 123–155. https://doi.org/10.1016/j.scitotenv.2012.04.028

Versteeg, H.K., Malalasekera, W., 2007. An introduction to computational fluid dynamics: the finite volume method, 2nd ed. ed. Pearson Education Ltd, Harlow, England ; New York.

Villette, C., Maurer, L., Delecolle, J., Zumsteg, J., Erhardt, M., Heintz, D., 2019. In situ localization of micropollutants and associated stress response in Populus nigra leaves. Environment International 126, 523–532. https://doi.org/10.1016/j.envint.2019.02.066

Villette, Claire, Maurer, L., Wanko, A., Heintz, D., 2019. Xenobiotics metabolization in Salix alba leaves uncovered by mass spectrometry imaging. Metabolomics 15, 122. https://doi.org/10.1007/s11306-019-1572-8

Vymazal, J., Dvořáková Březinová, T., Koželuh, M., Kule, L., 2017. Occurrence and removal of pharmaceuticals in four full-scale constructed wetlands in the Czech Republic – the first year of monitoring. Ecological Engineering 98, 354–364. https://doi.org/10.1016/j.ecoleng.2016.08.010

Wang, X., McCarty, P.L., Liu, J., Ren, N.-Q., Lee, D.-J., Yu, H.-Q., Qian, Y., Qu, J., 2015. Probabilistic evaluation of integrating resource recovery into wastewater treatment to improve environmental sustainability. PNAS 112, 1630–1635. https://doi.org/10.1073/pnas.1410715112

Yin, L., Wang, B., Yuan, H., Deng, S., Huang, J., Wang, Y., Yu, G., 2017. Pay special attention to the transformation products of PPCPs in environment. Emerging Contaminants 3, 69–75. https://doi.org/10.1016/j.emcon.2017.04.001

Figures and Tables

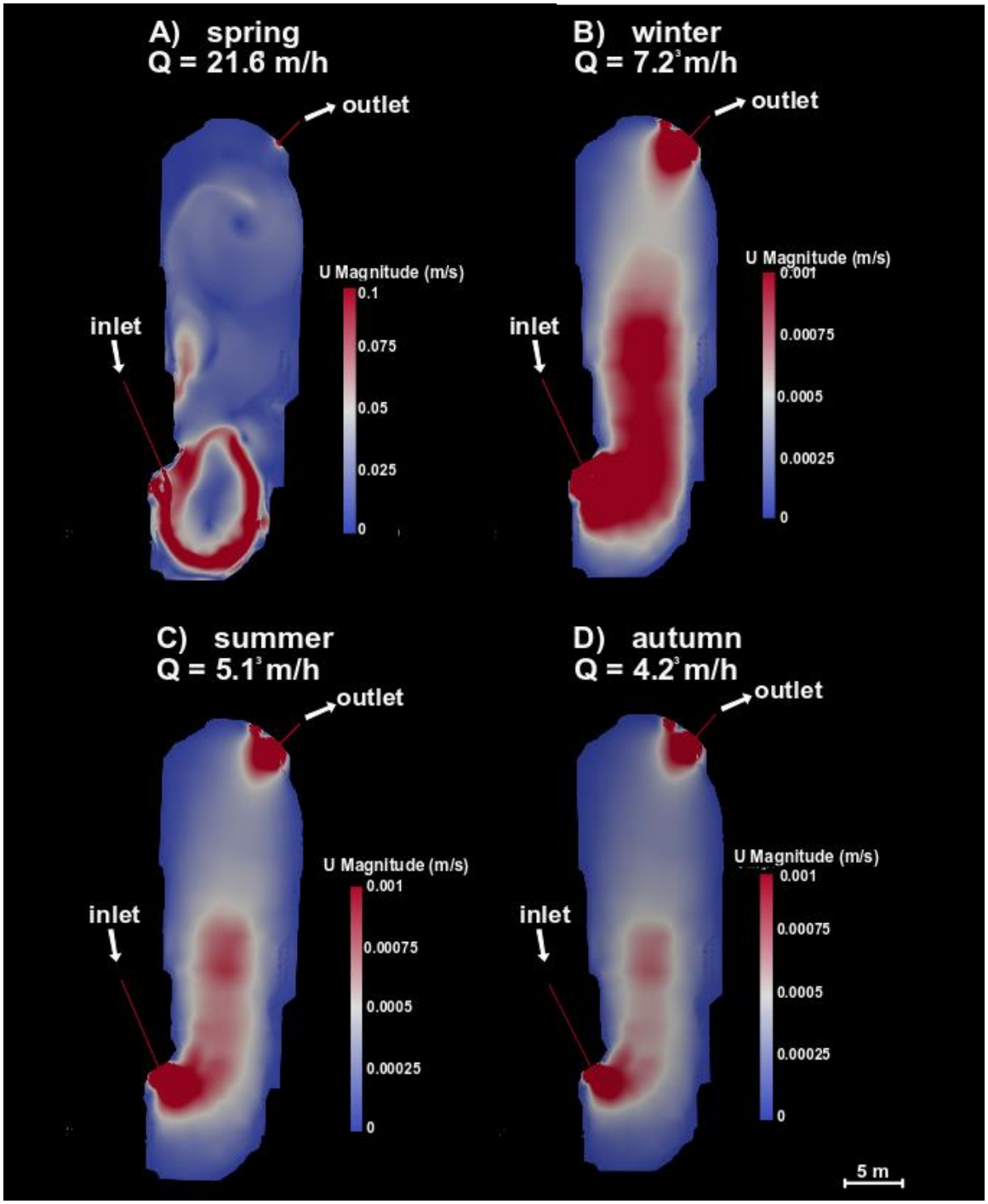

Figure 1. SFTW water flow in the different inlet flow rate conditions observed for each season. The water flow was simulated using the different conditions which have been

measured on the study site. The higher water flow monitored was about 21.6m^3/h and was simulated in the case A (spring). The conditions the most representative of average flow rate could be observed in cases B (winter with 7.2 m^3/h), C (summer with 5.1 m^3/h) and D (autumn with 4.2 m^3/h).

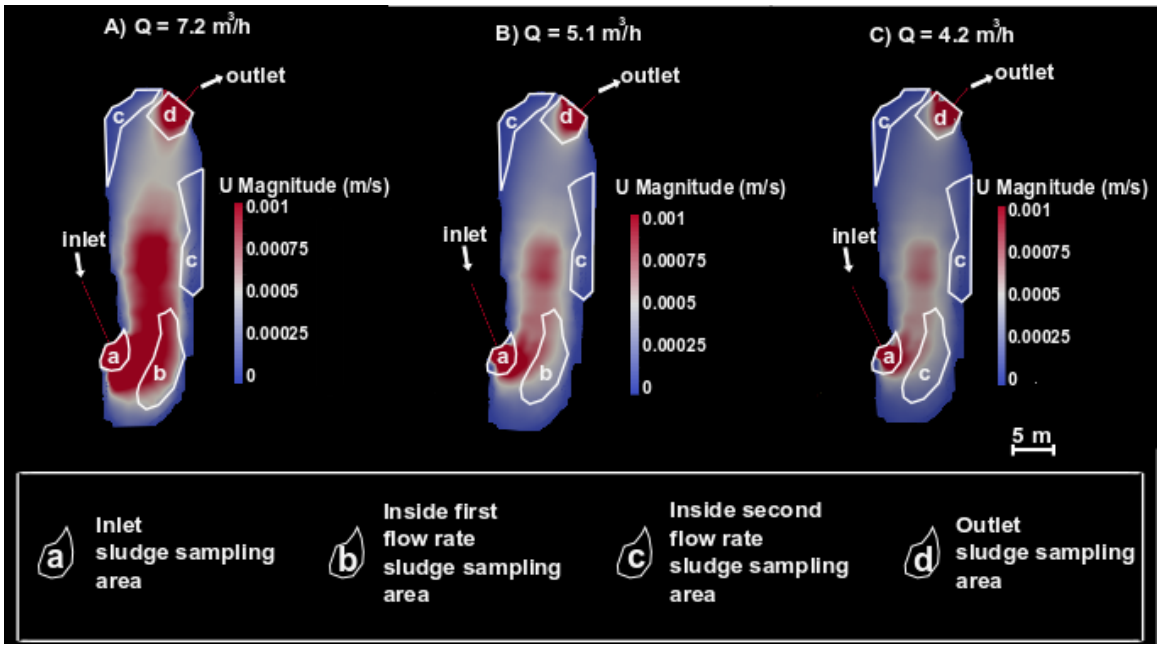

Figure 2. Water flow areas defining the sludge sampling strategy in the SFTW. Four areas based on similar water flow behavior were selected to collect sludge. The sludge areas were chosen to represent faster and slower water flow areas inside and at the system limits. Thus sludge was sampled at inlet and outlet areas (respectively area a and d), in relatively lower flow area (area c) and relatively higher flow area (area b) inside the SFTW. A) Sampling strategy applied with an inlet flow rate of 7.2 m^3/h. B) Sampling strategy applied with an inlet flow rate of 5.1 m^3/h. C) Sampling strategy applied with an inlet flow rate of 4.2 m^3/h. The spring simulation was not considered as it was not representative to the average conditions.

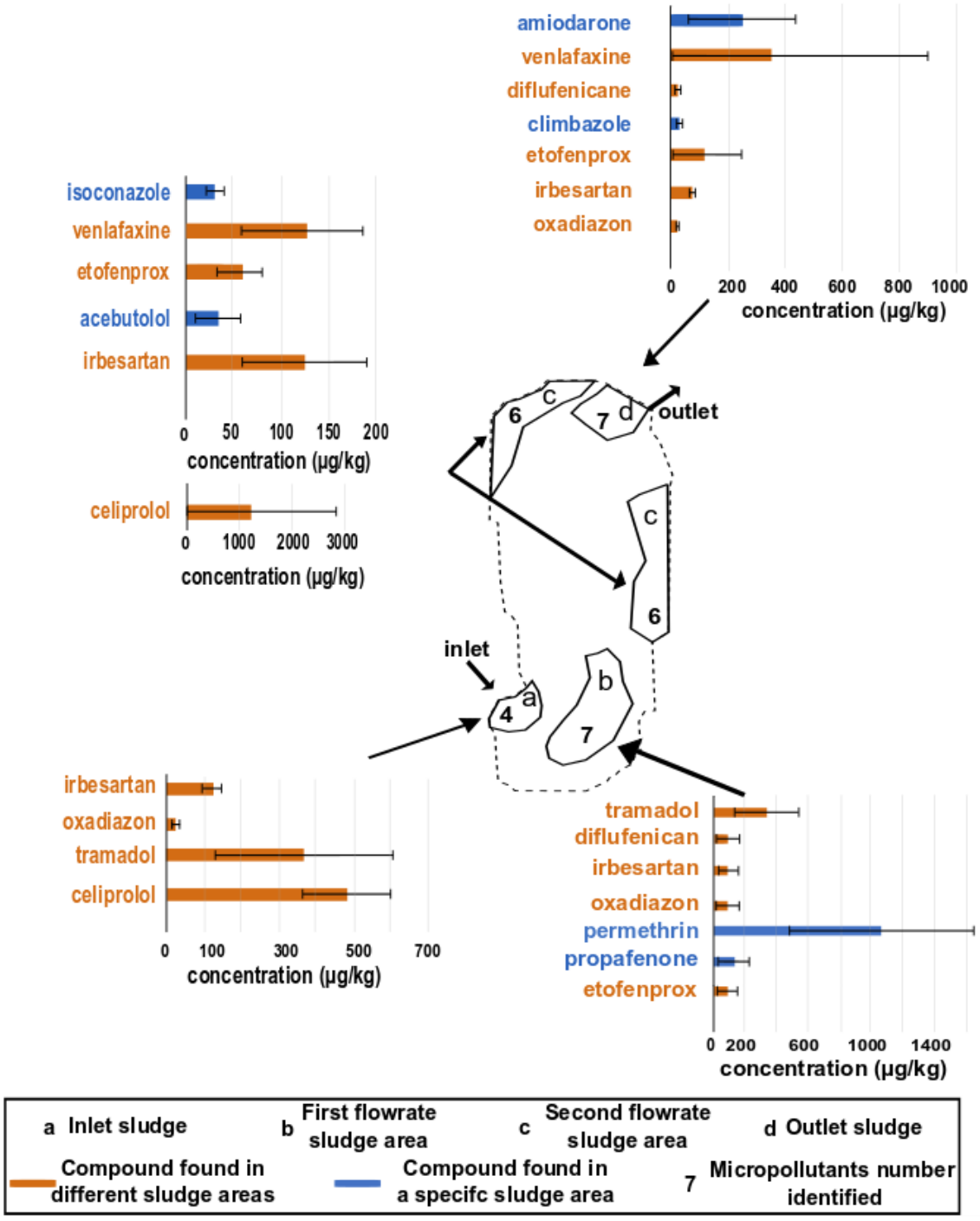

Figure 3. Distribution and quantification of micropollutants found for all seasons in the different flow rate areas of the SFTW. Compounds quantified were found in triplicates in each season. The concentration displayed shows the average concentration of all the samples; the standard deviation shows the concentration variability throughout the

seasons. Compounds found in different sludge areas (orange) were distinguished from those found specifically in a single area (blue).

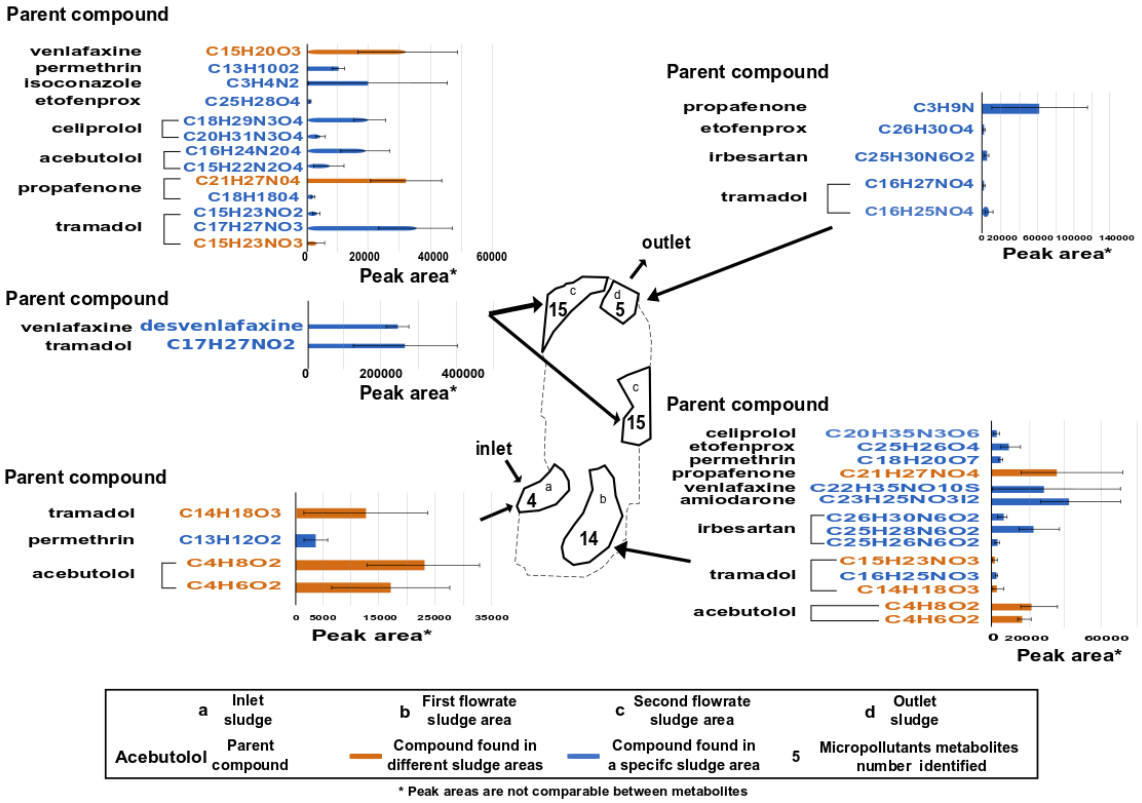

Figure 4. Distribution and intensity of micropollutants metabolites (catabolites and conjugated) found in each season in the different flow rate areas of the SFTW. The intensity displayed shows the average intensity of all the samples, the standard deviation shows the intensity variability throughout the seasons. All the samples were analyzed in triplicates for each season and standard deviation represents the intensity variation found through the seasons. Metabolites found in different sludge areas (orange) were distinguished from those found specifically in a single area (blue).

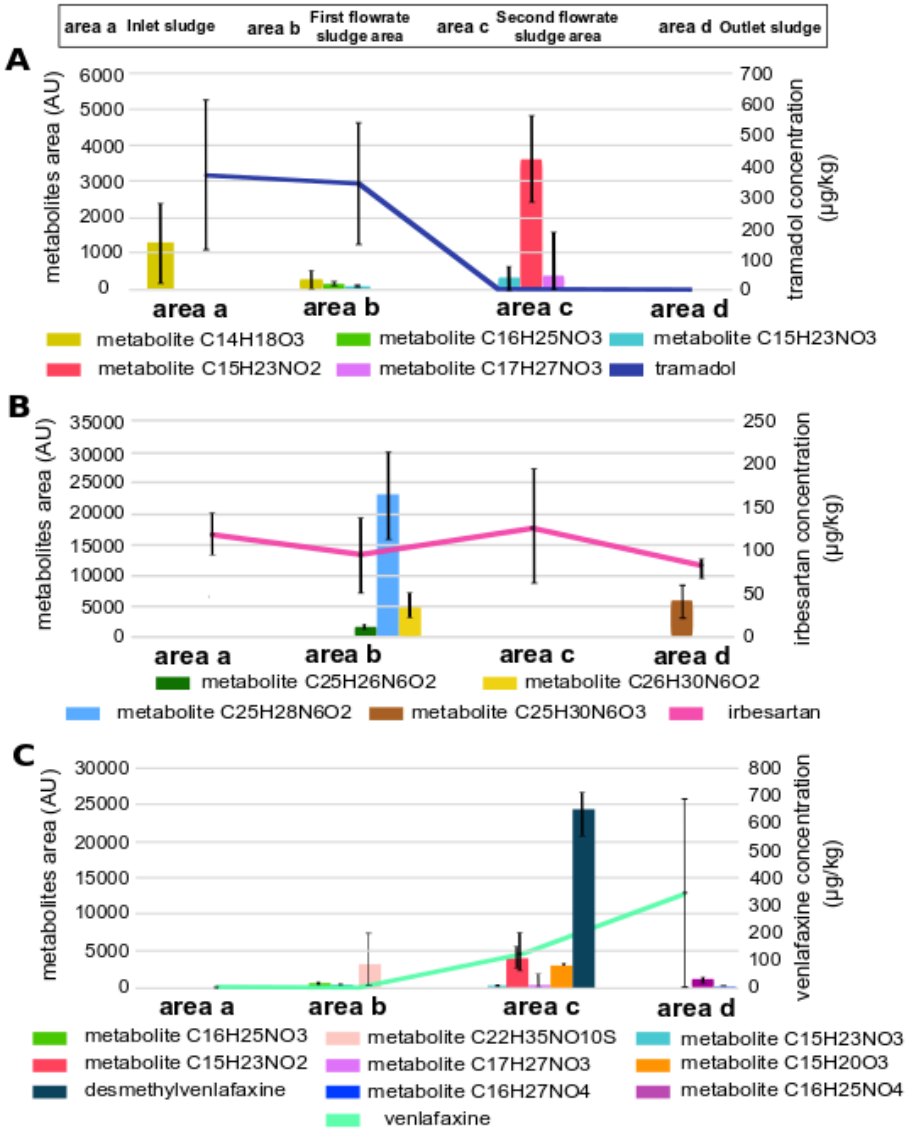

Figure 5. Distribution of tramadol, irbesartan, venlafaxine and their metabolites in the different flow rate areas of the SFTW. A, Tramadol and its metabolites found in the different areas. B, Irbesartan and its metabolites found in the different areas. C, Venlafaxine and its metabolites found in the different areas. The concentration of parent compounds, found at least in 2 areas, is not correlated to the water flow areas. Metabolites of these compounds are mainly (higher intensity and diversity) in the lower areas (b and c). All the analyses were performed in triplicates for each season and standard deviation represents the concentration/intensity variation found through the seasons.

.

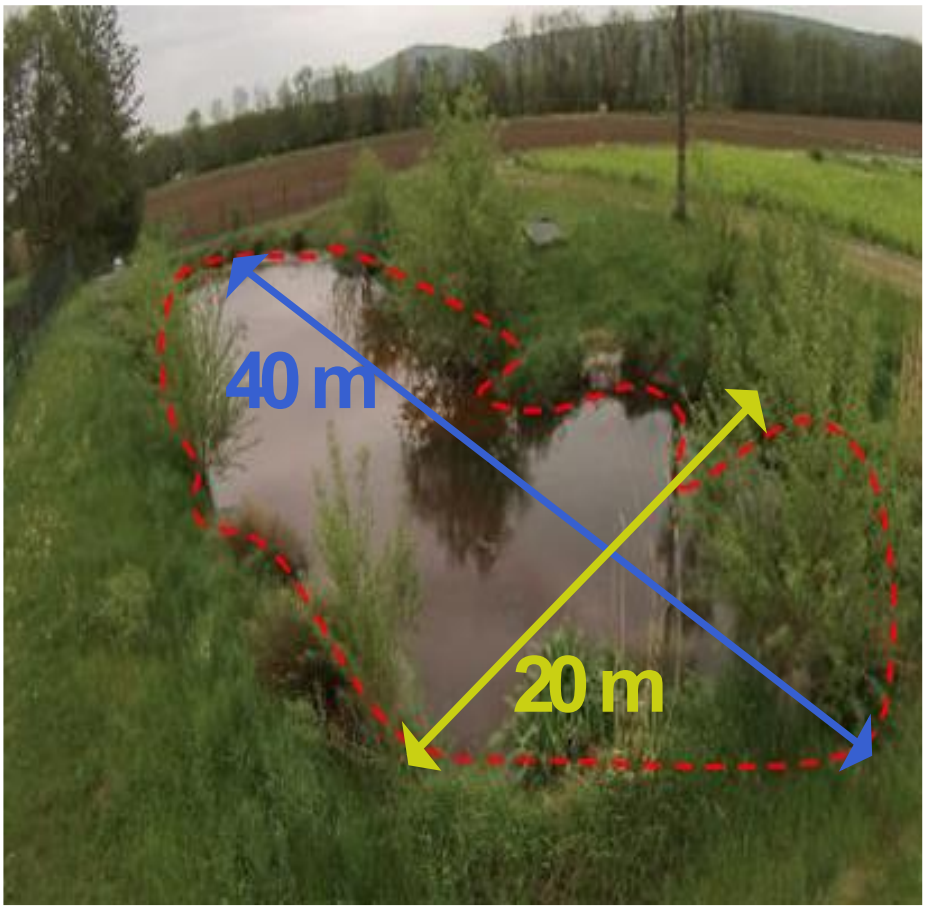

Figure S1. Photo from the SFTW located in the Lutter study site and its maximum lengths and width, which was used to build the 3D model.

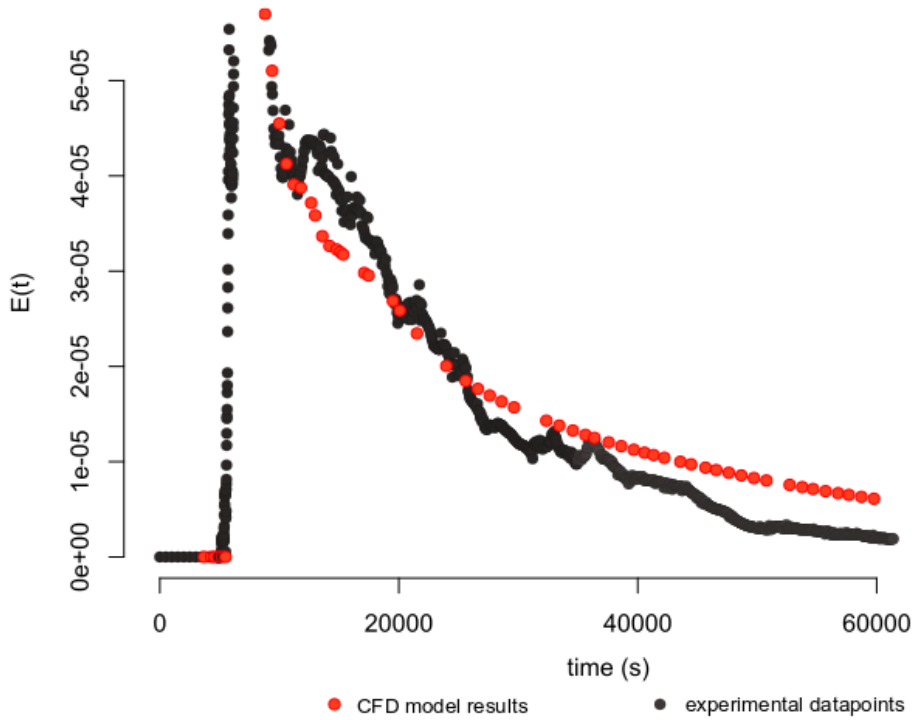

Figure S2. CFD model validation. Comparison of SFTW residence time distribution results found in the experimental field (black) and the simulated results (red)

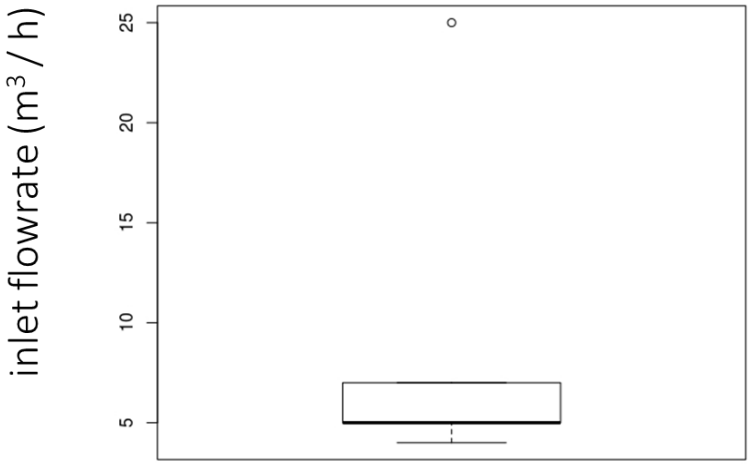

Figure S3. Inlet SFTW water flow distribution observed during two years on the study site.

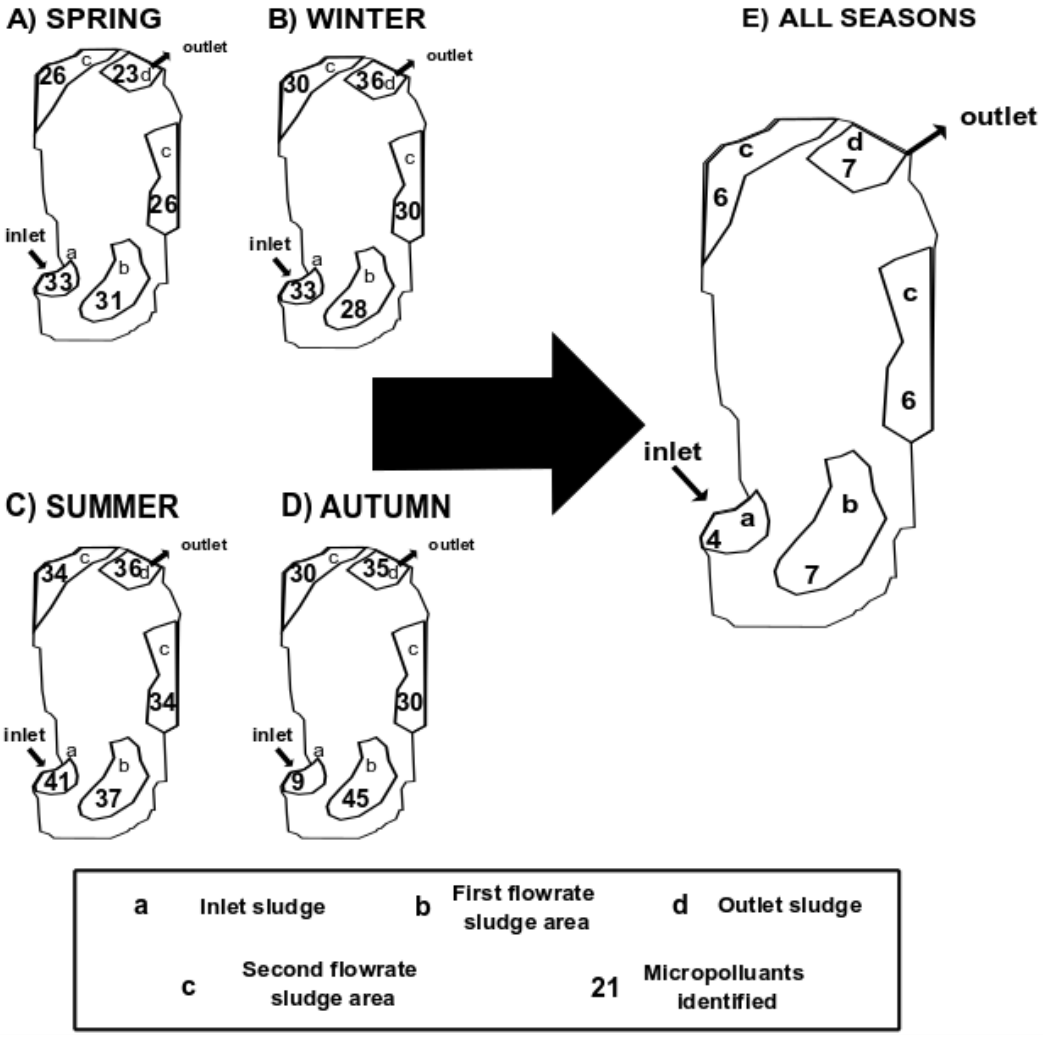

Figure S4. Micropollutants identified in triplicates in each area of the SFTW (inlet, 1st specific flow rate area, 2nd specific flow rate area and outlet). A) Compounds identified in the summer sampling, B) Compounds identified in the autumn sampling C) Compounds identified in the winter sampling D) Compounds identified in the spring sampling E) Compounds identified in all the sampling campaigns.

Dataset S1. Micropollutants identified in each sampling compartment (inlet, 1st specific flow rate area, 2nd specific flow rate area and outlet) for each sampling campaign.

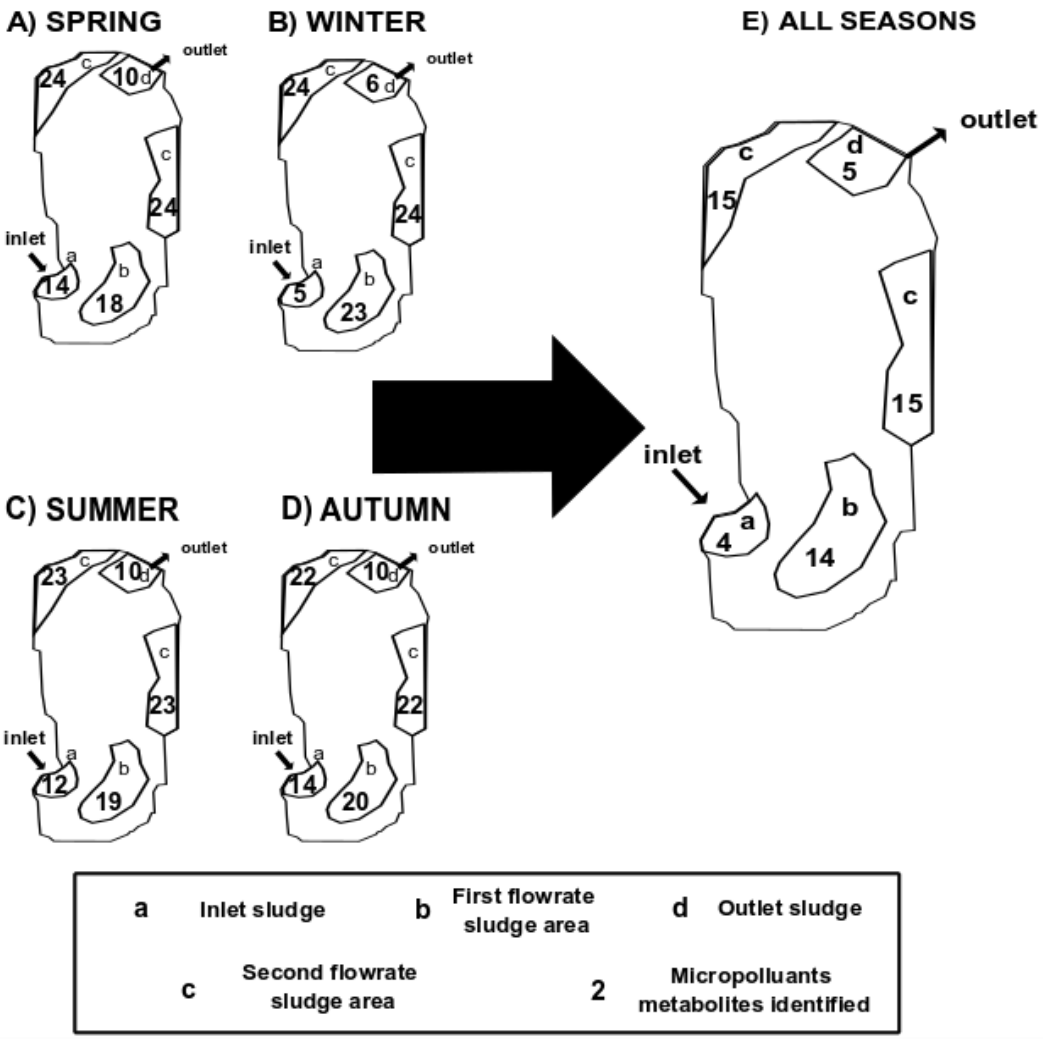

Figure S5. Micropollutants metabolites annotated in triplicates in each area of the SFTW (inlet, 1st specific flow rate area, 2nd specific flow rate area and outlet). A) Compounds annotated in the summer sampling, B) Compounds annotated in the autumn sampling C) Compounds annotated in the winter sampling D) Compounds annotated in the spring sampling E) Compounds annotated in all the sampling campaign.

Dataset S2. Micropollutants metabolites annotated in each sampling compartment of the SFTW (inlet, 1st specific flow rate area, 2nd specific flow rate area and outlet) for each sampling campaign.

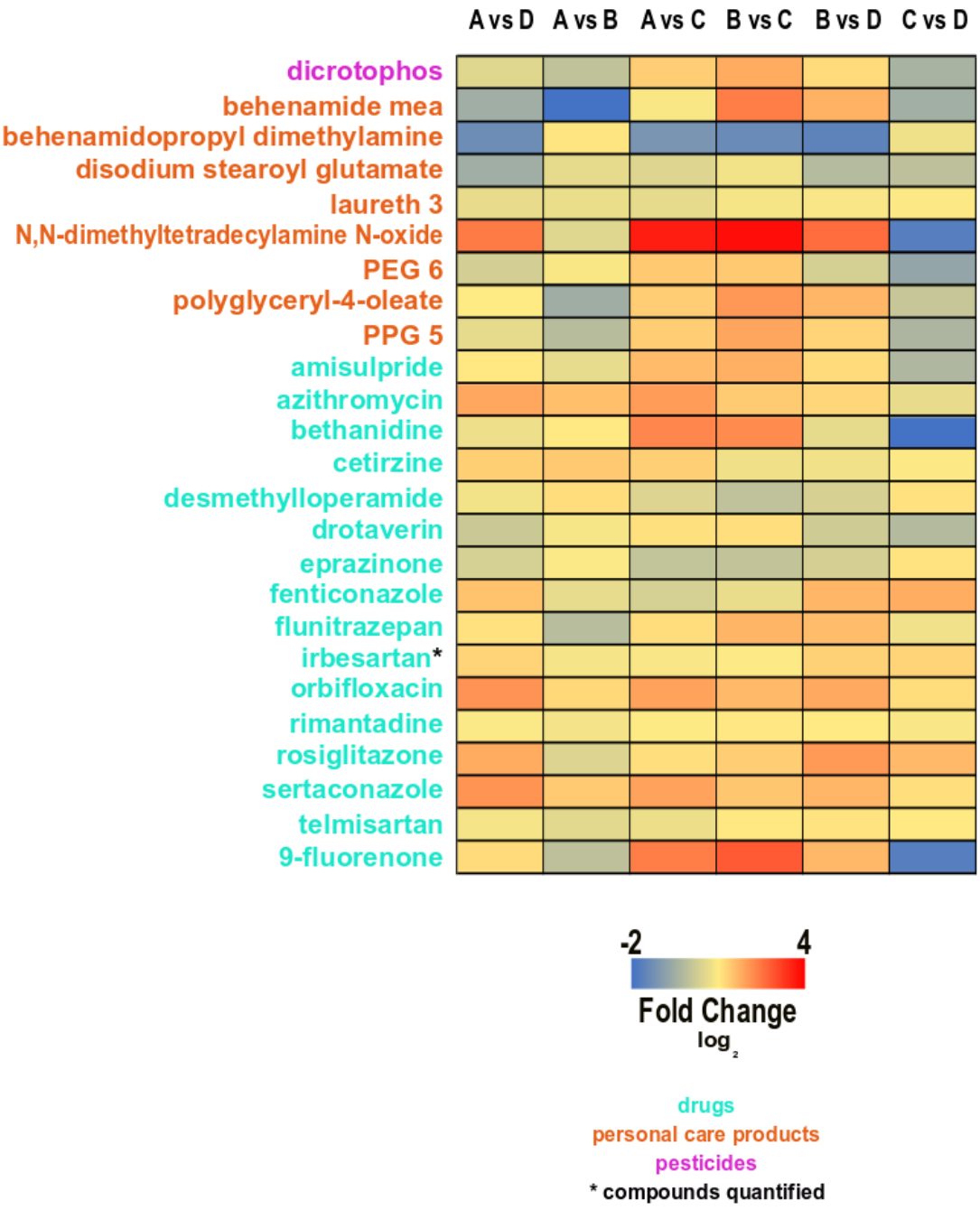

Figure S6. Heatmap of drugs, personal care products and pesticides found in each replicates from the different velocity field areas (A inlet, B intermediate and perpetual water flow, C low water flow, D outlet) using the log 2 fold change. The quantified compounds are characterized by a "*" mark.

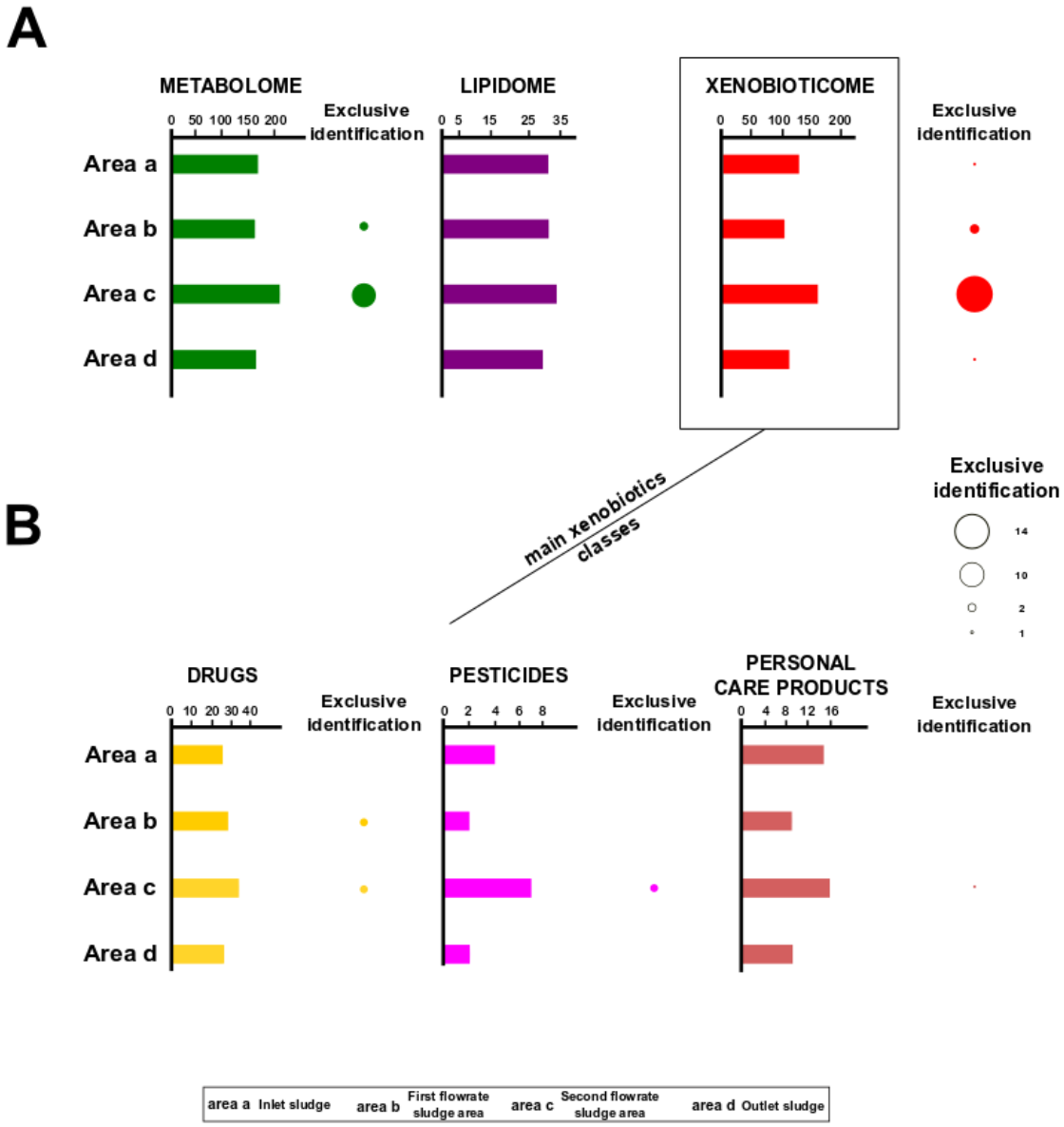

Figure S7. Plant metabolites, lipids and xenobiotics putative identifications and exclusive identifications (level 3 Schymanski) found in each replicates from the different velocity field areas (A inlet, B intermediate and perpetual water flow, C low water flow, D outlet). **A.** Identifications found in the main classes (plant metabolites, lipids, xenobiotics). **B.** Detail of the main xenobiotics classes identifications (drugs, pesticides, personal care products).

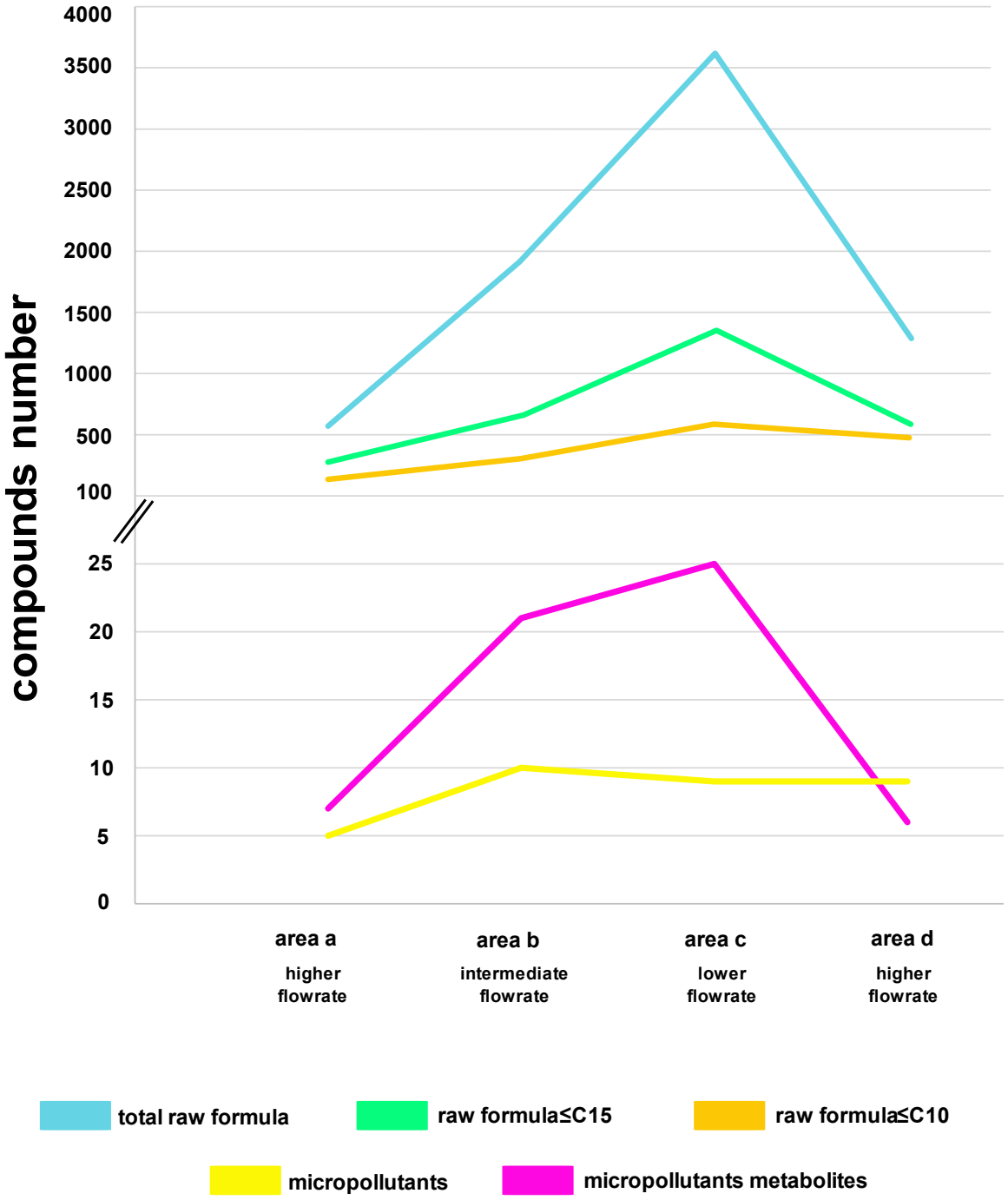

Figure S8. Compound distribution overview in the different sampling areas of the SFTW. Raw formula, raw formula with less than 15 carbons, raw formula with less than 10 carbons, micropollutants and micropollutants metabolites found in the 3 replicates for each sampling area.

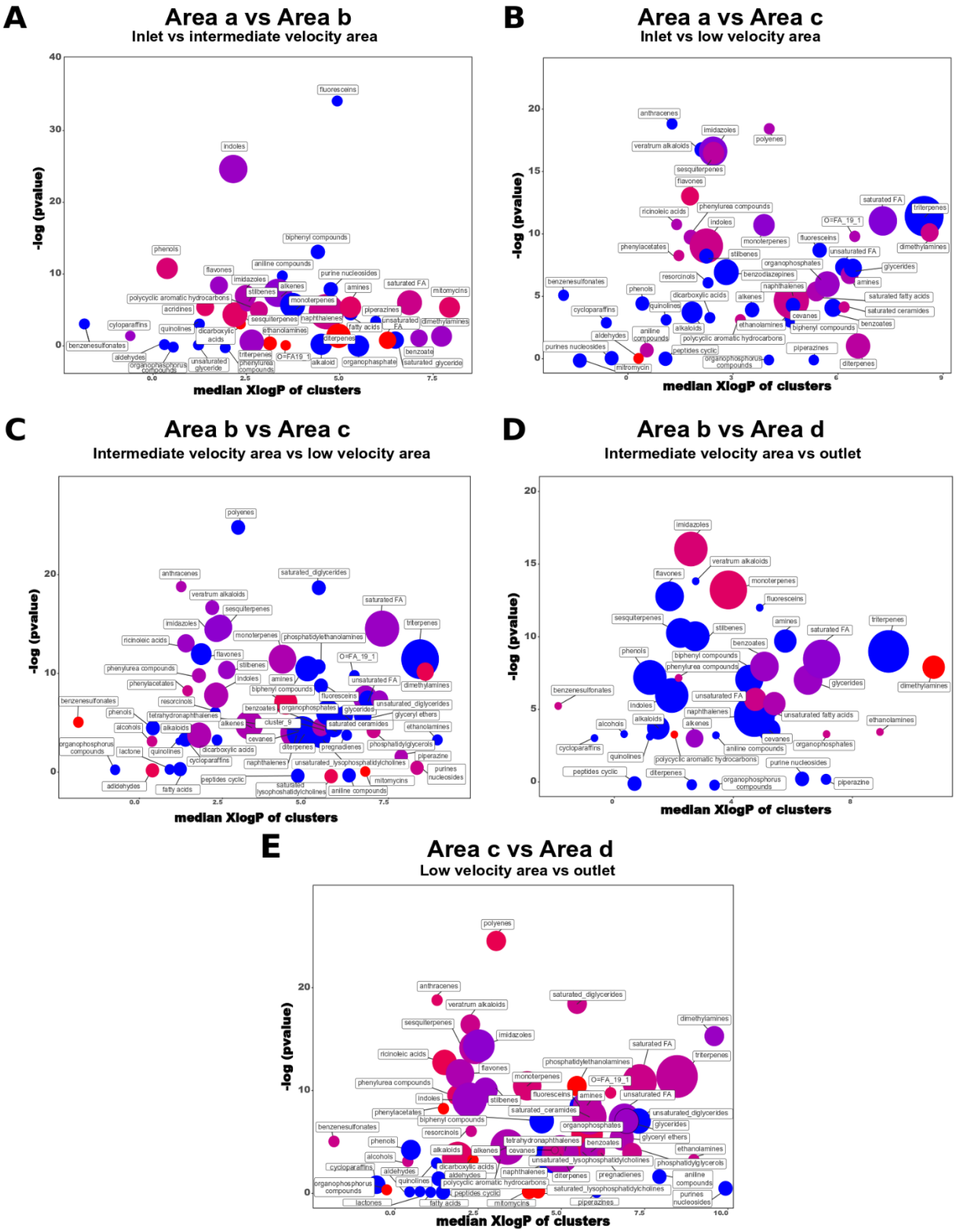
A
Area a vs Area b
Inlet vs intermediate velocity area
-log (pvalue)
median XlogP of clusters
B
Area a vs Area c
Inlet vs low velocity area
-log (pvalue)
median XlogP of clusters
C
Area b vs Area c
Intermediate velocity area vs low velocity area
-log (pvalue)
median XlogP of clusters
D
Area b vs Area d
Intermediate velocity area vs outlet
-log (pvalue)
median XlogP of clusters
E
Area c vs Area d
Low velocity area vs outlet
-log (pvalue)
median XlogP of clusters

Figure S9. Chemrich enrichment results found in the different wetland velocity field areas. A color gradient indicates the preferential area where the compounds were detected. **A**. Area A (inlet) and area B (intermediate and perpetual water flow) comparison. The red color indicates compounds classes mainly found in the area A, the blue those preferably found in the area B, and the purple those found in both areas (the shades is depending on the preferential area) based on the fold change (area A vs. area B). **B**. Area A (inlet) and area C (low water flow) comparison. The red color indicates compounds classes mainly found in the area A, the blue those preferably found in the area C, and the purple those found in both areas (the shades is depending on the preferential area) based on the fold change (area A vs. area C). **C**. Area B and area C comparison. The red color indicates compounds classes mainly found in the area B, the blue those preferably found in the area C, and the purple those found in both areas (the shades is depending on the preferential area) based on the fold change (area B vs. area C). **D**. Area B and area D (outlet) comparison. The red color indicates compounds classes mainly found in the area B, the blue those preferably found in the area D, and the purple those found in both areas (the shades is depending on the preferential area) based on the fold change (area B vs. area D). **E**. Area C and area D comparison. The red color indicates compounds classes mainly found in the area C, the blue those preferably found in the area D, and the purple those found in both areas (the shades is depending on the preferential area) based on the fold change (area C vs. area D).

A

Area A vs Area B

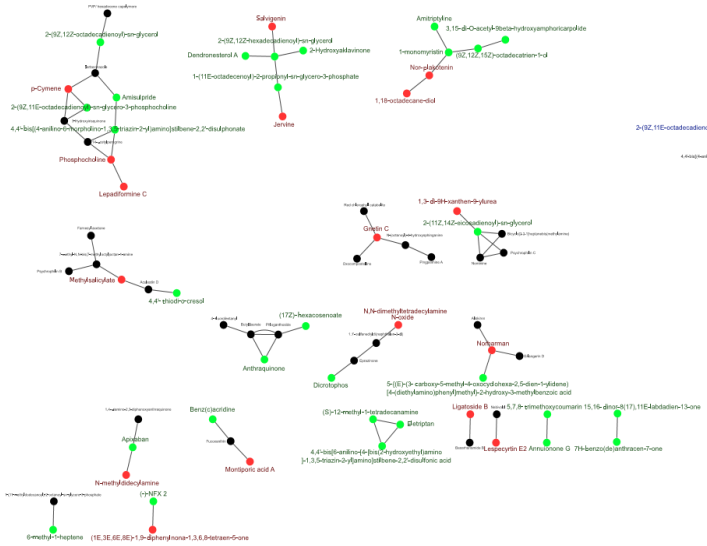

B

Area A vs Area C

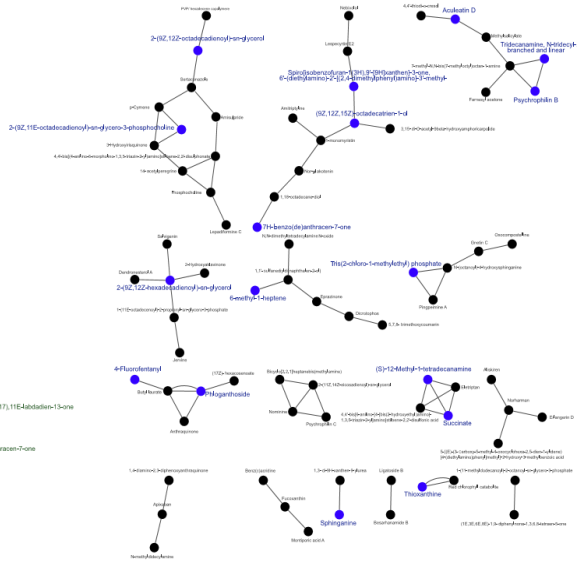

C

Area B vs Area C

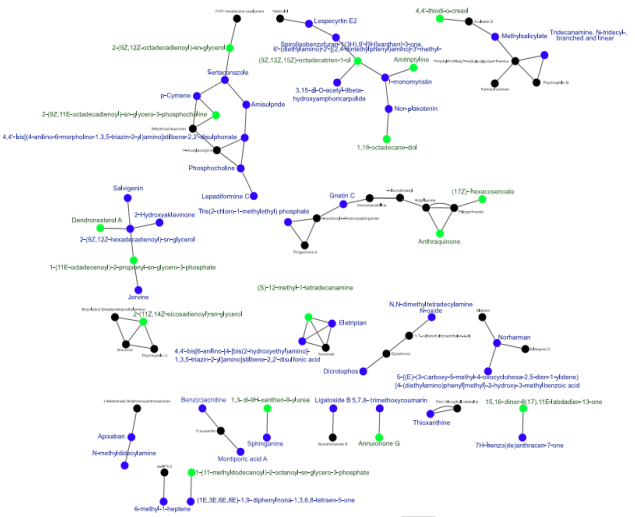

D

Area B vs Area D

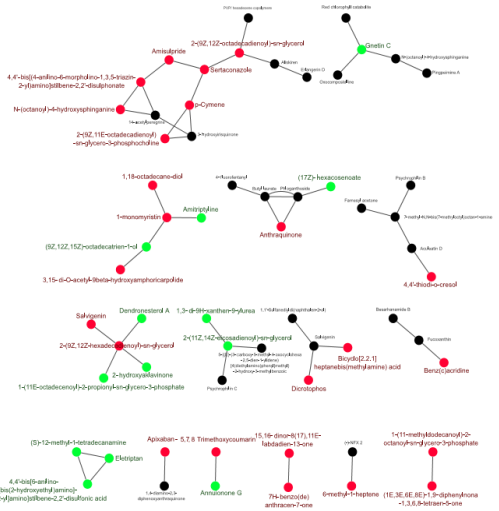

E

Area C vs Area D

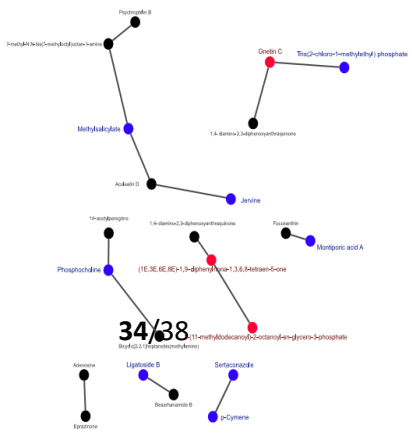

Figure S10. Metabolic network and biological pathways found in the different wetland velocity field areas using Metamapp and Cytoscape. A color gradient indicates the preferential area where the compounds were detected. Red compounds were preferentially found in higher velocity field areas (area A or area D: inlet or outlet). Green compounds were preferentially found in area B (intermediate and perpetual velocity field area). Blue compounds were preferentially found in area C (low velocity field area). Black compounds were found in both areas **A**. Area A (inlet) and area B (intermediate and perpetual water flow) comparison. **B**. Area A and area C (low water flow) comparison. **C**. Area B and area C comparison. **D**. Area B and area D (outlet) comparison. **E**. Area C and area D comparison.

Figure S11. Enzymes involved the metabolization of micropollutants in the different areas of the SFTW. The first- and second-generation enzymes are mentioned for each metabolite.

	pka	ionic fraction (%)	log Kow	solubility (mol/L)	molecular volume (cm^3)
acebutolol	9.65	1%	1.77	6.12e-3	301
amiodarone	8.47	8%	7.57	1.72e-6	408
celiprolol	9.66	1%	1.9	1.95e-3	341
climbazole	6.49	89%	3.83	1.48e-4	248
diflufenicane	9.03	2%	4.2	5.36e-7	274
etofenprox			6.9	1.68e-7	351
irbesartan	4.12	100%	5.3	4.06e-6	328
isoconazole	6.77	20%		1.02e-5	296
oxadiazon			4.9	5.97e-6	262
permethrim	-3.7	100%	2.88	4.34e-7	303
propafenone	9.63	1%	3.37	1.20e-3	311
tramadol	9.23	1%	3.01	3.03e-2	
venlafaxine	14.42	100%	3.2	2.14e-3	262

Table S1. Summary of pka, ionic fraction, log Kow, solubility and molecular volume of micropollutants found in the different water flow areas

Conflict of interest statement

The authors declare that they have no conflict of interest.